
# RADIATION EFFECTS ON AN ACTIVE YTTERBIUM-DOPED FIBER LASER

THESIS

Adam C. Poulin, Captain, USAF

AFIT-ENP-MS-16-M-079

**DEPARTMENT OF THE AIR FORCE**
**AIR UNIVERSITY**

***AIR FORCE INSTITUTE OF TECHNOLOGY***

**Wright-Patterson Air Force Base, Ohio**

AFIT-ENP-MS-16-M-079

MASTERS

THESIS

Presented to the Faculty

Department of Engineering Physics

Graduate School of Engineering and Management

Air Force Institute of Technology

Air University

Air Education and Training Command

in Partial Fulfillment of the Requirements for the

Degree of Master of Science

Adam C. Poulin, BS

Captain, USAF

March 2016

AFIT-ENP-MS-16-M-079

# RADIATION EFFECTS ON AN ACTIVE YTTERBIUM-DOPED FIBER LASER

Adam C. Poulin, BS
Captain, USAF

Committee Membership:

Lt. Col. Briana J. Singleton, Ph.D.
Chair

Lt. Col. Anthony L. Franz, Ph.D.
Member

AFIT-ENP-MS-16-M-079

# Abstract

This is the first published research focused on the impact of gamma and mixed gamma/neutron radiation on an actively lasing ytterbium-doped fiber laser. While the gain medium of the ytterbium-doped fiber laser was irradiated, the power was measured *in-situ* and the spectrum was recorded intermittently. Two radiation sources were used, a $^{60}$Co cell and a reactor. Three irradiation experiments were conducted per radiation source; pristine fibers were used for the first two experiments, and fibers from the second experiment were re-irradiated for the third experiment. The results indicate that as the total dose increased linearly with time, the laser experienced an exponential decay in power with a maximum power loss of 99.84% (at which time it was no longer lasing), and the lasing wavelength blueshifted up to 15 nm. The laser's initial power affects how much the radiation induced attenuation in the fiber. The laser, when exposed to 145 krad(Si), experienced less attenuation with a higher initial power than with a lower initial power. Power recovery experiments were conducted post-irradiation with the fiber laser off and actively lasing. Passively, the power recovered 100 and 550 $\mu$W in 18 and 90 hours respectively. Active recovery experienced the same 100 $\mu$W recovery in 9.3% of the time (10 min), and total power recovery of 12.6% and 4.4% for YDF1 and YDF2 respectively. The active recovery rate declined as the number of days following irradiation increased. This indicated a saturation of recovery after the less stable color centers were annealed. The active recovery rate for the re-irradiated fiber (gamma only) decreased 31% from the recovery rate just prior to re-irradiation.

# Acknowledgements

I would like to thank Lt. Col. Singleton for the help, ideas, and guidance she gave me during this process. She read each chapter of this thesis as it was completed, and provided me with constructive feedback. Thanks to Lt. Col. Franz who provided excellent tips to improve the visual layout of my charts, and prompted me to think more critically about my research and, ultimately, improve my level of understanding. Next, I would like to thank Dr. Nick G. Usechak at the Air Force Research Laboratory's Sensors Directorate. He lent me equipment from his lab to conduct my experiments, and provided lab space to use. He also took time from his very busy schedule to install the OSA code on my laptop, and ensure it was working properly. I would also like to thank 1st. Lt. Joseph Haefner at the Air Force Research Laboratory's Sensors Directorate. He spent numerous hours helping me in the lab with splicing, troubleshooting, and teaching me about fiber optics. He took time out of his day to help me, even though he was in no way obligated to do so. Next, I would like to thank the faculty at the Ohio State University's Research Reactor Lab for their assistance. The entire staff was extremely helpful in coordinating the schedule, setting up the experiments, and running the reactor. They were a pleasure to work with. Finally, I would like to thank my girlfriend. Your support through this time was what I needed to make it through all the stress and frustration. You pushed me to stay on task and get things done. You never complained about editing my thesis, and you helped make it clear and concise.

Adam C. Poulin

# Table of Contents

Page

# List of Figures

Figure Page

# List of Tables

MASTERS

# 1. Introduction

## 1.1 Motivation

Since the 1980s, fiber optics have been the workhorse for the long-distance telephone network. Fiber optics are still a staple in communication networks today, and they have been implemented in other areas such as astronomy, medicine, and space. Fiber optics are not only thinner and lighter than metal wires, but they also possess greater bandwidth and less susceptibility to interference, and transmit multiple signals through the same fiber. These properties result in systems being lighter, more compact, and more robust than their metallic predecessors.

The advantages of fiber optics have been furthered through the development of doping silica with rare earth (RE) elements. Compared to standard fiber optics, RE-doped fibers provide signal gain within the fiber, reducing and sometimes eliminating the need for massive electronic amplifiers within a communication network or on a satellite where space and weight come at a high price. The advancement of RE-doping techniques has allowed much greater doping concentrations of RE elements to be achieved, resulting in shorter lengths of fiber to be used for some applications. However, even at low RE-doped concentrations, RE-doped fibers can be employed as integral parts in fiber amplifiers and lasers.

To date, the most common RE element used in fiber optics has been erbium (Er) [1]. Er-doped fibers (EDFs) have dominated in the communication world as a result of their ability to amplify signals of commonly used communication wavelengths

(1330 and 1550 nm) [2]. However, the concentration to which Er can be doped is limited. The formation of ionic clusters increases with higher levels of Er-dopant concentrations, and reduces the functionality of the Er-doping. If the ionic clusters form in a large enough area, the signal gain, due to the RE-dopant, can become too concentrated in one part of the fiber and leads to a breakdown of the fiber from excessive heat. However, the concentration barrier faced by Er-doping has been surpassed by concentration levels achieved with ytterbium (Yb)-doping, on the order of $2.4\times10^{22}$ $cm^{-3}$, along with the use of other co-doping elements [1].

The use of Yb is widespread because of its simple energy-level diagram, large delta of functional wavelengths, and high luminescence efficiency [3]. Yb-doped fibers (YDFs) exhibit high output power, excellent efficiency, versatility in complex and unstable environments, and minimal losses from excited state absorption and concentration quenching [4]. Ytterbium-doped fiber lasers (YDFLs) are utilized in several applications including high-powered lasers and optical amplifiers. Even at low doping concentrations, Yb-doped fiber amplifiers (YDFAs) and YDFLs are capable of producing gain. Additionally, Yb can be doped at a much higher concentration level than Er, allowing for higher gains in shorter lengths of fiber. YDFs have become the most important of the RE fibers, and have proven to be less susceptible to radiation damage compared to other RE-dopants [5]. However, in order to achieve a high level of doping, aluminum (Al) must also be co-doped into the silica in order to prevent the Yb from forming ionic clusters within the fiber.

The doping of silica with RE elements provides many excellent attributes, but not without some setbacks. RE-doped fibers are more susceptible to radiation damage than standard telecommunication optical fibers typically by orders of magnitude [6]. Since RE-doped fibers are increasingly being used in harsh environments where radiation is present, it is important to understand how these

fibers will perform under these circumstances. The need for research regarding the radiation sensitivity of RE-doped fibers has been specifically identified in multiple publications [7, 8, 9]. Data on the radiation sensitivity of RE-doped fibers is essential for the appropriate utilization of these fibers in space applications. Numerous studies have shown that fibers exposed to radiation produce color centers within the matrix of the fiber. A color center, also known as an F-center, is formed when an anion (a negatively charged ion) is displaced from the host lattice and is replaced by an electron. Color centers can occur naturally in compounds if they are heated to very high temperatures or they can be created by irradiation in fibers that are doped with RE ions. In either case, sufficient energy was deposited into the host material to remove an anion in the lattice, leaving a positive net charge, or hole, in its place. An electron is then attracted to this hole and then binds to the lattice. This binding of the electron causes absorption of light, especially in the visible spectrum. Although, these color centers can also absorb the pump or signal light from a fiber amplifier or fiber laser causing a reduction in transmitted signal through the fiber [10]. This linear absorption through the fiber can be measured at the wavelength of interest in decibels (dB) per unit length, and is characterized as radiation-induced attenuation (RIA). This degradation from light absorption, specific to RE-doped fibers, is thought to affect three main mechanisms associated with the absorption of energy. These mechanisms will be discussed in the next chapter on theory.

RE-doped fibers are more susceptible to radiation than pure $SiO_2$ fibers. Numerous studies have indicated that these types of fibers can be hardened for protection against the RIA that develops within the fibers during irradiation. Some studies suggest that the radiation sensitivity of the fiber is more dependent on the concentration of secondary, co-doped elements (such as Al, Ge, or P) rather than

the concentration of RE-dopants [6]. While co-doping the fiber with some elements can increase the radiation sensitivity of the fiber, there are other elements, or combinations of elements, that can decrease the radiation sensitivity of the fiber (this is known as hardening the fiber). Specifically, a few studies reported that Cerium/Yb or Er/Yb co-doped fibers resulted in radiation hardening of the fibers [4, 11, 12]. YDFs have shown less RIA compared to EDFs exposed to the same amount and type of radiation, meaning YDFs are less susceptible to radiation damage. Additionally, EDFs that were co-doped with Yb were less sensitive to radiation than EDFs with no co-dopant. In all cases, it has been shown that the RE-doped fibers are the most radiation sensitive part of the system (amplifier or laser for example) they are in [5, 12, 13, 14].

It is difficult to predict or model how any one type of fiber will perform under the exposure of radiation and, therefore, radiation sensitivity should be determined experimentally [6]. There has been a great effort in cataloging the many different types of fibers to determine their radiation sensitivity and usability in environments with radiation. Among these efforts are two large databases on fiber characteristics for space and radioactive environments. One database is maintained by the NASA Electronic Parts and Packaging (NEPP) Program, and the other database is managed by the European Space Agency's European Space Components Information Exchange System (ESCIES) [15, 16]. These databases are paramount for selecting the best fiber in which the following are considered: the radiation levels to which it will be exposed and the amount of shielding it requires. In spite of these large databases, which were built upon data from multiple experiments on fibers and fiber systems, no studies have been performed on active YDFLs, one study has been performed on an active Er-doped fiber laser *in-situ*, and only a handful of studies have been conducted on the radiation damage of actively operated fiber

amplifiers *in-situ* [2, 11, 17, 18, 19]. In Singleton's dissertation she points out "there are scant published results on the radiation effects to Yb-doped fiber laser systems while in the active mode" [2]. Others have specifically expressed the desire to see radiation experiments performed with active configurations or just more experiments on YDFs in general [18, 20, 21]. A separate paper discusses the desire to know the "worst case" for RIA with each type of doped fiber amplifier or laser configuration [22]. Thus, the motivation for this work was to publish results of an active YDFL as it was irradiated to determine how the radiation affected the laser.

## 1.2 Problem Statement

The goal of this thesis was to determine the affect of gamma and mixed gamma/neutron radiation on the power output of an active YDFL. To my knowledge, these are the first and only documented experiments of an active YDFL being irradiated with data taken *in-situ*. The experiments focused on monitoring power measurements and spectral data of the YDFL *in-situ* while being irradiated. The two sources used were both housed at the Ohio State University Nuclear Reactor Lab (OSU-NRL). The first was a gamma only radiation source from a $^{60}$Co irradiation cell, and the second was a continuous mixed gamma/neutron radiation source from the Ohio State University Research Reactor (OSURR). The analysis from the experimental data will focus on comparing the RIA observed in the YDFL with previous experimental data on other irradiated RE-doped fibers and fiber systems which use RE-doped fibers as a gain medium. This information will help to determine how the RIA of an actively operated YDFL will be affected by radiation in comparison to the RIA of RE-doped fibers and fiber systems from previously conducted experiments.

# 2. Theory

## 2.1 Origin of Fiber Optics

Fiber optics operate by utilizing a phenomenon known as Total Internal Reflection (TIR). TIR occurs when light travels inside a medium that has a higher index of refraction than the medium surrounding it. When the light hits the boundary of the two mediums, the light is reflected back into the medium, essentially trapped within that medium. Historically, TIR was not mentioned much until 1841 when Daniel Colladon, a Swiss physicist, began demonstrating it in his scientific lectures [1]. He essentially used a water cooler with a spout at the bottom to guide light from a light source (see Figure 1). The light could be seen traversing down, totally encompassed inside the waterfall. By the early 1900s, scientists were utilizing TIR in glass rods to guide light to illuminate microscope slides. However, fiber optics did not really begin to shine until the 1960s, when the first lasers were built. Even then, it took another decade to discover a way to produce glass pure enough to transmit signals over 500 meters with at least 10% of the signal light remaining. In today's fibers, it is possible to transmit signals further than 50 kilometers with 10% of the original light signal remaining [1].

TIR operates by trapping light within a medium that is surrounded by a material with a lower index of refraction. For fiber optics, the material in which the light will be guided through (or trapped) is called the core, while the material that surrounds the core is called the cladding. The most common material used for the core and the cladding is glass; although, the core and cladding must have different indexes of refraction in order for TIR to occur. The difference in indexes of refraction is accomplished during the manufacturing process of the glass. The core and cladding indexes of refraction can differ by as little as 1% (1.485 for cladding, 1.5 for core)

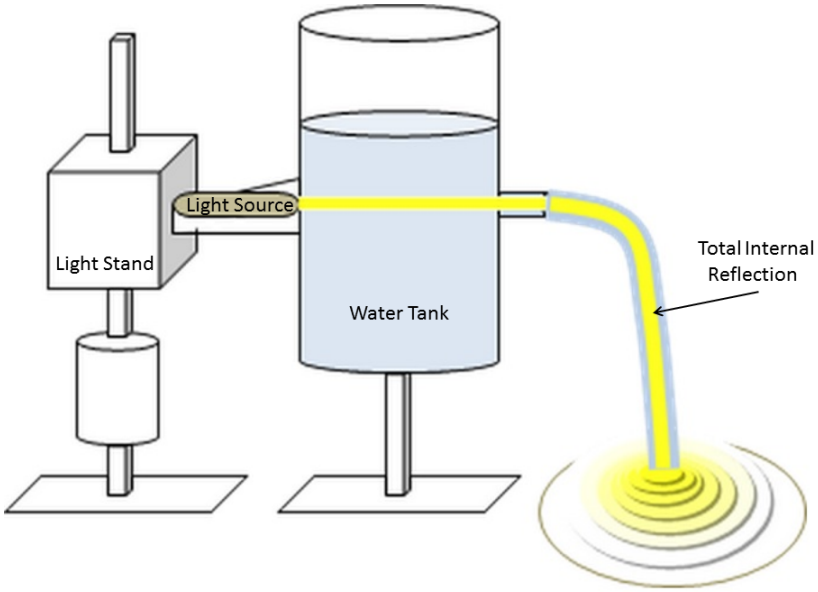


**Figure 1. In essence, the total internal reflection demonstration conducted by Daniel Colladon in the 1840's [23].**

and TIR will still occur. The main principle of TIR can be seen using Snell's law,

$$n_I \sin(\theta_I) = n_T \sin(\theta_T), \tag{1}$$

where $n_I$ and $n_T$ are the indexes of refraction for the core and cladding respectfully, and $\theta_I$ and $\theta_T$ are the incident and transmitted angles. Snell's law shows that in order for the light to be trapped within the core, $\theta_I$, must be an angle that makes $\theta_T$ greater than 90°. The critical angle, $\theta_{crit}$ , is defined as the angle of $\theta_I$ when $\theta_T$ will equal 90°. In order to have total internal reflection, $\theta_I$ must exceed the critical angle. The critical angle can be found by setting $\theta_T = 90$ degrees and solving for $\theta_{crit}$ using equation (1).

$$\theta_{crit} = \arcsin\left(\frac{n_T}{n_I}\right) \tag{2}$$

As previously stated, the usual difference in indexes of refraction between the core

and cladding is about 1%. Therefore, $n_T/n_I = 1.485/1.5 = 0.99$. From this, the critical angle of a fiber can be determined.

$$\theta_{crit} = \arcsin(0.99) = 82^\circ$$

Once the signal or pump light is coupled into the fiber, the light will travel through the fiber reflecting itself back into the fiber each time it encounters the boundary between the core and cladding.

Glass is a non-crystalline solid, and can be made from multiple compounds (as long as the crystallization of the compound can be stopped by rapid cooling or other techniques) [1]. In fiber optics, the most commonly used compounds are oxides, and the most prevalent oxide used is $SiO_2$. However, $SiO_2$ must be highly purified in order for it to be useful in modern fiber optics. The attenuation of glass is the major limiting factor for use in fiber optics. Glass used in fiber optics experience attenuation from 1 dB/m, which limits the distance at which the light will travel. At this attenuation, the light can only travel in the glass fiber a few kilometers before the signal will be too small to detect. The attenuation comes from impurities in the $SiO_2$ which absorb light in the 0.6 to 1.6 $\mu$m range. These impurities are iron, copper, cobalt, nickel, manganese, and chromium. When the impurity levels of these elements are reduced to 1 part per billion, a more useful form of $SiO_2$ is attained [1]. This highly purified form of $SiO_2$, known as silica, has a much lower attenuation level around 5 dB/km. Both the core and the cladding are typically made with silica. However, an entire fiber made of pure silica, would not exhibit TIR, since the core and the cladding would both have the same indexes of refraction ($\approx 1.45$ for pure silica). Therefore, in order to make the entire fiber from silica, the core, the cladding, or both the core and the cladding must be doped with other elements in order to alter their optical properties.

## 2.2 RE-doped Optical Fibers

Dopants such as germanium, aluminum, and phosphorus are used to raise the index of refraction of silica [24, 25]. Only a few dopants have been found to lower the index of refraction of silica; the most typical dopant is fluorine, followed by boron [1]. Other dopants, such as RE metals are doped into silica to provide signal gain within the fiber, allowing the fiber to ultimately be used as an amplifier or laser. The RE element used in doping will determine the fundamental characteristics of the fiber. Some of these characteristics will determine the wavelengths at which the fiber can be pumped, the signal wavelengths the fiber will amplify, as well as other non-optical consequences such as radiation sensitivity. However, in order to understand how the fiber will be affected by the RE element, the RE elements themselves must first be understood.

As Digonnet explained, rare earth elements are divided into two groups each containing 14 elements. The first group, the actinides, does not contain any stable isotopes, so they are not used in fiber optics. The second group, the lanthanides, has many stable isotopes that are utilized in optical amplifiers and lasers. The most electronically stable of these ions is the trivalent (3+) level of ionization. The electronic makeup of these isotopes is the xenon structure ($5s$ and $5p$ electron shells filled) plus a varying number of $4f$ electrons (1-14) [25]. The filled $5s$ and $5p$ electron shells act as a shield against the $4f$ shell. As the number of $4f$ electrons increases (corresponding to an increase in atomic number), the electrons become more tightly bound to the nucleus. This increases the shielding effect of the outer $5s$ and $5p$ electron shells, causing useful characteristics in the trivalent isotopes when incorporated into bulk materials. One useful characteristic is that the energy levels of the lanthanides remain nearly unaltered, which allows for few host-induced splittings when doped into another material. Next, they exhibit little or no

vibrational excitation from the host lattice, and minimal non-radiative relaxation (phonon transitions). Finally, because of these characteristics, the $4f$ optical transitions exhibit narrow, weak bands, and highly efficient emissions [25]. From the $4f$ shell, the electrons can transition from different excited and ground states as they absorb photons (i.e. pump signal). Due to the frequencies needed to transition these $4f$ electrons, the photon wavelengths that are absorbed are in the visible and infrared spectrum. Conversely, for lasers, these same wavelengths will be emitted from stimulated emission when a signal of the same wavelength encounters an excited $4f$ electron.

$Yb^{3+}$ ions possess properties that make it an excellent dopant for fiber lasers and amplifiers. $Yb^{3+}$ demonstrates high luminescence efficiency, and the ability to amplify light over a broad range of wavelengths (975 to 1200 nm). These properties allow for a variety of uses in fields such as telecommunications, medicine, and military applications [3]. Because $Yb^{3+}$ ions can be doped to much higher concentration levels than $Er^{3+}$ ions, this allows for higher gains in shorter lengths of fiber. However, in order to achieve this high level of doping, aluminum oxide ($AlO_2$) must also be co-doped into the silica in order to prevent the $Yb^{3+}$ ions from forming clusters within the fiber, which decreases the amplification of the fiber. While the $AlO_2$ co-dopant provides the ability to increase the $Yb^{3+}$-doping concentration in the silica, it also negatively affects the fiber by increasing its radiation damage susceptibility. However, the benefits of greater concentrations of $Yb^{3+}$ ions outweigh the increased radiation damage susceptibility. Also, YDFs have proven to be less susceptible to radiation damage compared to other RE-doped fibers [5]. YDFs also exhibit high output power, excellent efficiency, and decreased losses from excited state absorption and concentration quenching due to Yb's relatively simple energy level diagram (see Figure 2) [4]. These favorable characteristics (especially when

considering making a laser) have made YDFs the most important of the RE-doped fibers.

When $Yb^{3+}$ is doped into silica, the energy levels of $Yb^{3+}$ are broadened from phonon interactions with the silica matrix. These broadened Stark levels (splitting of one level into multiple sub-levels) can be seen in Figure 2 and show that the ${}^2F_{7/2}$ level has split into four sub-levels and the ${}^2F_{5/2}$ level has split into three. The $Yb^{3+}$ ions in silica can absorb photons at specific wavelengths and can emit photons at other specific, yet longer wavelengths as well. These transitions promote the efficiency of the YDFL because they create levels that will absorb and decay at frequencies close to the pump and signal frequencies. These are the main properties of the RE elements that have propelled fiber optics to the forefront of technology today.

### 2.3 Laser Principles

Electrons in an atom are bound to the electric field of the nucleus. The electrons occupy certain orbitals around the nucleus depending on their energy. Each orbital around a nucleus has a discrete energy level that an electron must posses in order to occupy a specific orbital. As an electron increases its orbiting distance from the nucleus, its energy increases but its stability decreases. Electrons prefer to be in the lowest energy configuration possible where they are considered to be stable. When a photon is incident on a material, an electron in the material can absorb the photon. The photon must have the specific energy to raise the electron to a higher orbital (energy level) in order to be absorbed. If it does, the electron will absorb the photon and be excited to a higher energy level, shown as $E_2$ in Figure 3. The electron will only remain excited for a short period of time, as little as nanoseconds, before it will relax to its lower, stable energy level, $E_1$ [27]. When this lowering of

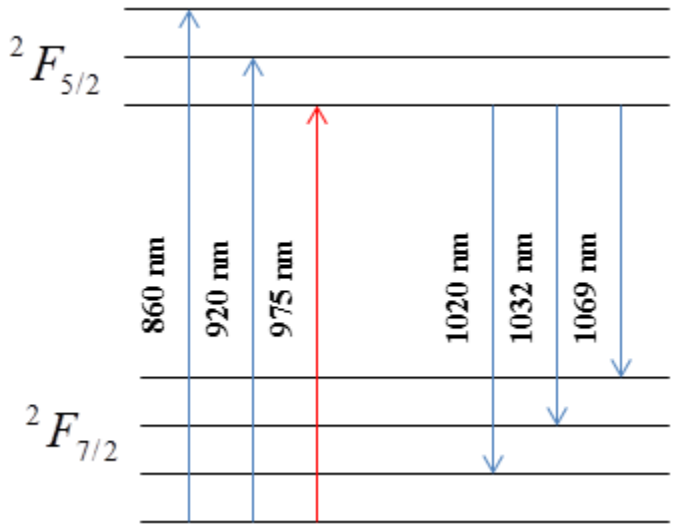


**Figure 2. The energy level diagram of $Yb^{3+}$ doped in silica. The lasing wavelength utilized in this thesis is not shown here specifically. This is due to the fact that this diagram is for $Yb^{3+}$ doped in silica only. When other co-dopants are added to the silica, the energy level spacing can change slightly from the co-dopants interacting with the lattice of the silica. This image was recreated from [26].**

energy occurs, a photon is emitted with a frequency, $\nu$, which is proportional to the energy difference of the two energy levels.

$$E_2 - E_1 = h\nu,$$

where $h$ is Planck's constant. This process, where the excited electron relaxes to its lower energy level without any external influence, is called spontaneous emission (see "Spontaneous emission" in Figure 3). The photon released from spontaneous emission can be emitted in any direction and with any phase. Stimulated emission occurs when an electron is in an excited state, then is stimulated into a lower energy state by a photon. When this stimulated emission occurs, the electron releases a photon that is the exact match to the photon that caused it to decrease its energy level. Now there are two photons with the same frequency, phase, polarization, and propagation direction [27]. This is shown in Figure 3 (Stimulated emission). If there

are enough excited electrons in the material stimulated emission will again occur, twice this time since there are now two photons in the system. These two photons will create two more photons via stimulated emission, then the four will create four more, and so on. This cascading effect is optimized to create gain of a specific frequency which in turn produces a powerful coherent beam of light, called a laser.

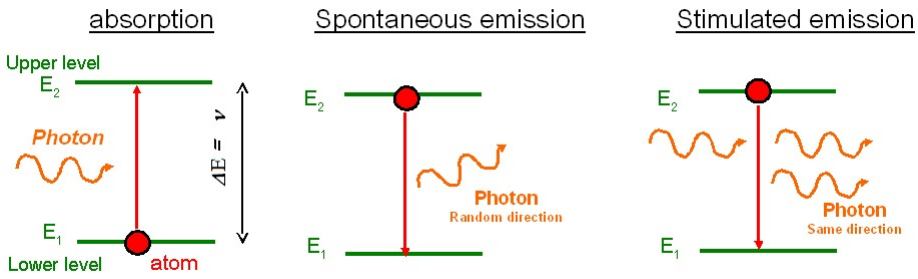


**Figure 3.** ***Absorption:*** **an incident photon with energy equal to $\Delta E$ excites the electron to the upper level.** ***Spontaneous emission:*** **The excited electron relaxes to lower level as it releases a photon with random direction, phase, and polarization.** ***Stimulated emission:*** **The excited electron is stimulated to the lower level by an incoming photon. When the excited electron transitions to the lower level, it releases a photon with the exact frequency, phase, polarization, and propagation direction as the incoming photon [28].**

Lasers operate by utilizing the principles of absorption and stimulated emission to create gain, but the electrons in the material used for lasing (gain medium) must be carefully prepared. A laser must have a continuous chain reaction of stimulated emission in order to keep lasing. This is accomplished by constantly exciting the electrons in the gain medium to an excited state, so that the number of excited electrons in the material is greater than the number of electrons in the lower energy states. This is called population inversion. Population inversion can be achieved by constantly barraging the electrons with photons of the specific frequency needed to excite them to a higher energy level. In this thesis, this was accomplished by using a pump laser tuned to 975 nm to excite the electrons to the desired excited energy level (specifically level 3 as seen in Figure 4). Yb is able to be made into a laser by

exploiting the multiple Stark levels in the upper ${}^2F_{5/2}$, essentially turning a two-level system into a three-level laser. This is accomplished as the electrons are pumped to a higher energy state in the ${}^2F_{5/2}$ level, $E_3$, then relax without releasing a photon (non-radiative relaxation) to the lowest ${}^2F_{5/2}$ energy level, $E_2$. Once here, the electrons can transition by stimulated emission to the ground state in the lower ${}^2F_{7/2}$ energy level, $E_3$. This process is depicted in Figure 4.

### 2.4 Ytterbium-doped Fiber Lasers

The YDFL for the experiments presented in this thesis will operate by exciting electrons in the YDF, the gain medium, with a laser. This laser, called a pump laser, is tuned to the wavelength of 975 nm which will specifically excite the ${}^2F_{7/2}$ level electrons to the ${}^2F_{5/2}$ level. After a short time there will be more electrons in the ${}^2F_{5/2}$ level than in the ${}^2F_{7/2}$ level, creating a population inversion in the YDF. Some of the excited electrons will then spontaneously decay, as mentioned above, releasing photons as this occurs. However, the wavelengths of the released photons will vary depending on which energy level the electrons relax to, creating a number of photons with many different wavelengths, directions of propagation, and phases. Some of these photons that are released from spontaneous emissions will then trigger stimulated emission with the other excited electrons within the YDF, granted the photons have an angle of incidence greater than the critical angle (keeping them inside the core of the fiber). This is a welcomed process for photons of the desired wavelength, the signal or signal wavelength, but an unfortunate byproduct when triggered by the random photons (photons not at the signal wavelength). The random photons are multiplied as they stimulate emissions from other excited electrons during spontaneous emission. This process, called amplified spontaneous emission (ASE), creates a broad range of wavelengths that is amplified

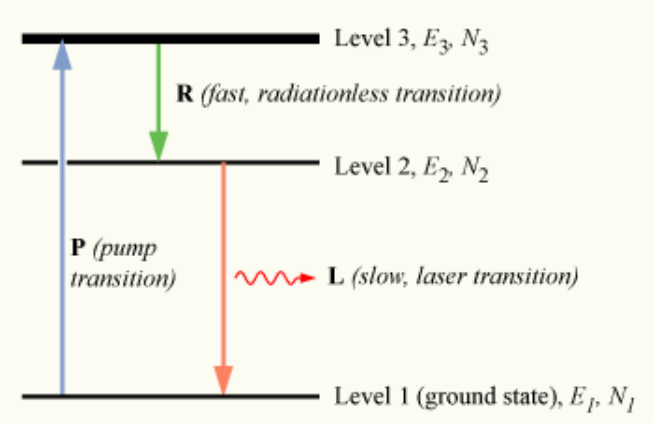


**Figure 4. The electron is excited to the third energy level. Then it relaxes to the second energy level without releasing a photon (non-radiative relaxation), and finally relaxes to the ground state through stimulated emission (lasing) [29].**

within the YDF. ASE reduces signal gain (of the desired wavelength) by decreasing the number of excited electrons (through stimulated emission) as these random photons propagate through the YDF in all directions. ASE creates signal distortion and is a large source of noise for YDFLs [2].

Some lasers have an external signal source to start and maintain the process of stimulated emission for the desired wavelength of the laser. These sources are often lasers themselves, since lasers are coherent, powerful, and easily tunable to specific wavelengths. For the YDFL used in these experiments, the YDF is pumped high enough so that the electrons are able to spontaneously emit enough photons at the signal wavelength to create a strong, coherent signal within a few round trips of the ring laser. This process can be expedited with the addition of an optical isolator in the ring laser. The optical isolator only allows the propagation of light in one direction, so the photons generated by spontaneous emission and ASE will only be allowed to pass through the optical isolator if they are traveling in the forward direction of the ring laser. After a couple of round trips through the ring there will be more photons traveling in the forward direction than in any other direction. These photons will act as the signal light, which will begin the cascading effect of

stimulated emission to produce a coherent beam of light at the signal wavelength. The desired signal wavelength for this thesis is 1060 nm. With the addition of an output coupler, 75% of the signal within the ring laser will be coupled back into the ring to keep the stimulated emission process running, while 25% of the signal will be directed to the power meter for measurements.

## 2.5 Components of Ytterbium-doped Fiber Laser

This experimental set-up requires a number of complex fiber optic components including: connectors, t-couplers, tree couplers, wavelength division multiplexers, and optical isolators. Without these components a coherent light beam cannot be created from just fiber optics. They work together to produce this coherent beam by isolating the signal photons (1060 nm), and by denying photons at other wavelengths from reentering the gain medium. This ensures that the majority of photons entering the YDF on successive trips around the ring are at the signal wavelength. This allows for a large gain of signal wavelength while keeping gain at other wavelengths to a minimum. The design, integration, and operation of these components will be discussed.

In order for light to transfer from one fiber to another the light has to exit from the end of the source fiber and couple into the end of the receiving fiber. The transfer of light from the source fiber to the receiving fiber with minimal loss is not an easy task. This requires precise techniques so that the light can be guided into the core of the receiving fiber where it will continue to transmit as it was before the junction. An example of this is the ferrule connector (FC). The FC is made by first removing the plastic coating, which protects the silica in the fiber, at the end of the fiber. The exposed silica at the tip of the fiber is then cleaved, polished, slid into a ceramic ferrule, and glued into place. Then a metallic connector is placed over the

ferrule to allow for easy connections to other FCs through a mating sleeve. The mating sleeve allows for the ends of the two fibers to come in contact with each other in a precisely controlled manner by screwing the FCs into the mating sleeve. There are a few different types of FCs that are commonplace in fiber optics. However, for the experimental setup in this thesis, the FCs were restricted to the angled physical contact (APC) type [1, 30].

For the FC/APC type, each end of the fiber is cleaved with an angled cut and then polished with superfine sandpaper. The cleaved angle reduces back reflections when the light exits the source fiber and couples into the receiving fiber. Each connector from the source and receiving fibers are screwed in at opposite ends of a mating sleeve. The mating sleeve allows for both fiber cores to come in contact with each other, stabilizes them so that the light can transfer from one fiber to the next, and ensures the angled portions of each fiber are properly aligned with one another [1]. These connectors work well for transferring the signal from one fiber to another, but sometimes more complex components are needed in order to alter the signal in specific ways.

The coupler allows the light to be split from one or more fibers into another fiber or fibers. Couplers that split light into two separate fibers are called t-couplers. Tree couplers, on the other hand, are couplers that split light into three or more fibers. These are just two types of couplers, out of many types, on the market today. For the construction of the YDFL used for this thesis, only one type of coupler was used, the t-coupler (or sometimes referred to as y-coupler as it better describes how it actually looks) [1]. The t-coupler typically has an input fiber and two output fibers. With the YDFL built for the experiments conducted in this thesis, t-couplers (each labeled as "Output Coupler" in Figure 6) were used in three places. These t-couplers allowed for the incoming light to be split into two separate

output fibers at varying percentages. This YDFL setup, for example, used a 99/1 coupler, a 50/50 coupler, and a 75/25 coupler. These numbers describe the percentage of input signal that each of the output fibers will transmit and, therefore, must total 100%. For the construction of the YDFL, the t-coupler that was connected to the WDM allowed for a small portion (1%) of the pump signal to be directed to a second t-coupler (50/50 coupler). This 50/50 coupler split the pump signal in half so the power and spectrum of the YDFL could be monitored and recorded. The third t-coupler was used to siphon off 25% of the signal wavelength from the ring laser and direct it into a power meter to record the power.

Unlike the connectors, where the ends of the fibers are placed in contact with one another to transfer the light, couplers are made by placing the fibers in parallel with one another. The plastic coating and cladding are removed from one side of the fibers in the coupler, and brought into contact with one another [1]. Then, the fibers are heated so that they fuse with each other. Another technique involves stripping both fibers down to the core, twisting the fibers around one another, and then fusing them together. This helps to increase the transfer of light between the fibers. The fibers are stretched while being fused in order to alter how the transmission of the signal is divided between the outputs. This method is called the fused-fiber process.

The wavelength division multiplexer (WDM) is similar to a t-coupler, but it will separate the input signal into two different wavelengths rather than a division of total power. This is done by a few different methods, but the most common method uses interference filters. Interference filters, also known as dielectric filters (since they are typically made from dielectrics which do not conduct electricity), are made by placing two materials with different indexes of refraction in alternating thin layers. The difference in the index of refraction creates reflections at the boundary of the two layers. As the interference filter increases in thickness (more alternating

layers added), the reflection of light from the filter also increases due to an increased number of boundaries to cause reflections. The light that is not reflected at these boundaries, and therefore transmitted, can be tuned by selecting the proper thickness of the layers of dielectric material [1]. The formula for calculating the transmitted wavelength, $\lambda$, or determining the proper thickness of the dielectric material, $D$, is given by

$$N\lambda = 2nD\cos\theta.$$

Where N is an integer, n is the index of refraction of the dielectric, and $\theta$ is the angle of the incident light with respect to the normal. Fiber Bragg gratings can also act as a WDM, however, there is a difference between this method and the interference filter method. Interference filters allow a specific wavelength to be transmitted through the filter, while fiber Bragg gratings reflect specific wavelengths. For this experiment, the WDM was used in reverse from how it was described previously. Therefore, the WDM combined the signal from the pump laser with the signal from the ring (1060 nm) into the output fiber of the WDM [1].

Finally, the optical isolator, as the name implies, isolates light traveling in a certain direction by obstructing light not traveling in the desired direction from passing through it. The allowed direction of travel, the clockwise direction in this case, is depicted in Figure 6 by the arrow in the box representing the isolator. Typically, isolators are used to prevent feedback in laser cavities such as the ring laser used in these experiments. The isolator works by first collimating the incoming light with a lens. The light then travels through an input birefringent crystal. This crystal has its ordinary polarization direction on the vertical axis (o-ray = 0°), and its extraordinary polarization direction on the horizontal axis (e-ray = 90°). This crystal causes the light to split it into two different beams with two different

polarizations. Next, the two beams pass through a Faraday rotator that rotates the polarization of both beams by 45° changing the o-ray to 45° and the e-ray to -45°. Now, the e-ray and o-ray have polarizations that are rotated such that the output birefringent crystal recombines the two beams into one, and passes it through the output of the fiber optical isolator. This happens because the output birefringent crystal is chosen such that its o-ray polarization is 45°and its e-ray polarization is -45°. When the two beams each match their respective e or o-ray with the crystal, they get recombined into one beam and can then propagate out of the isolator. This case is represented in the top of Figure 5 (blue ray). However, if light enters the optical isolator from the output, attempting to propagate through it in the reverse direction, very little light, if any, will get through to the other side. This happens because the output birefringent crystal (on the right side) splits the incoming light into two separate beams, again, both with different polarizations (o-ray to 45°and the e-ray to -45°). Then, the two beams propagate through the Faraday rotator, and each beam's polarization is rotated again by 45°. Now the o-ray is polarized to 90°and the e-ray is polarized to 0°. When these beams travel through the input birefringent crystal, their polarizations are oriented 90° different from the crystal's o and e-rays. Therefore, the crystal further separates the beams and prevents either of the beams from propagating through the input of the isolator [31]. This can be seen at the bottom of Figure 5 (red ray).

## 2.6 Radiation Effects on RE-doped Fibers

Radiation can degrade the performance of fiber amplifiers or lasers by the formation of color centers in the host material (silica). Color centers can be created by a variety of processes. The three main mechanisms responsible in the creation of color centers involve the lattice of the silica being disturbed or changed from the

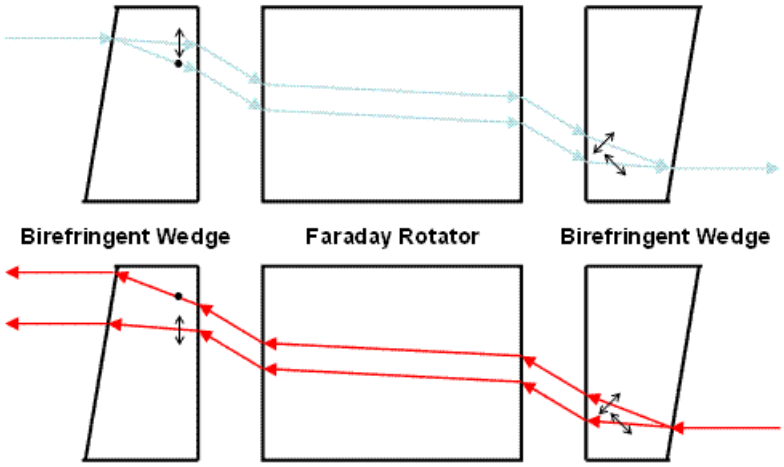


**Figure 5. Light propagating through a fiber optic isolator. The isolator allows light to propagate from left to right (top) but blocks light from traveling right to left (bottom) by using two different birefringent crystals and a Faraday rotator [31].**

energy deposited by the radiation. Oxygen atoms can be displaced from their standard position in the lattice, causing an oxygen deficiency (vacancy defects); excess oxygen atoms can be moved into abnormal positions within the lattice (impurity interstitial defects) [2]; the double bond between the silicon and oxygen atoms in silica can be broken (dangling bond defects). All of these radiation induced defects cause absorption of light within the core of the fiber.

Of these, the most common process that creates color centers is a type of oxygen deficiency defect. This specific color center is created when an anion is removed from its normal position in the lattice of the silica and a hole (positive charge) is left in its place. This hole then attracts and traps an electron. The trapped electron couples to the vibrations in the lattice causing absorption at specific wavelengths [32]. These vibrational absorptions can absorb the pump or signal light, reducing the transmitted signal through the fiber [10]. This linear absorption through the fiber is characterized as RIA. RIA is measured by comparing the difference in absorption before and after irradiation, at the wavelength of interest in decibels (dB) per unit length [2].

The absorption of light is thought to be from three main mechanisms that interact with the Yb ions in the fiber. First, the color centers reduce efficiency of energy transferred from the pump wavelength to the stimulated emission wavelength by absorbing both the pump and signal light [17, 33]. Consequently, the reduction in power conversion leads to a reduced output power of the amplifier/laser. Next, non-radiative transfer of energy can occur from the pumped RE atoms to impurities in the fiber, if the excited ions are located close to the impurity site. Lastly, the impurities in the fiber can absorb the signal light causing a reduction in transmission [2]. The presence of RE-dopants in silica induces a susceptibility to radiation damage. Silica alone does not exhibit much RIA from radiation. However, if it is doped with other elements, the damage becomes pronounced.

For a thorough review of previous radiation studies conducted on Yb, Er, and Yb/Er-doped fibers see section 2.7 of Singleton's dissertation "Radiation Effects on Yb-doped Fibers" [2]. There, she highlights 13 separate studies, three of which were conducted on active fibers. In Singleton's study on the irradiation of an active Yb-doped fiber amplifier, she concluded that the defects in the YDF induced by radiation caused interference with the excitation and de-excitation of the $Yb^{3+}$ ions. This was shown by the nominal decrease in transmission of the pump signal within the YDF, but the transmission loss of the signal through the YDF was significant. It was this transmission loss from the absorption of signal light by the radiation defects in the silica that dominated the loss of gain within the Yb-doped fiber amplifier.

## 2.7 Active Recovery (Annealing)

The formation of color centers within the YDFL cause absorption of the pump and signal wavelengths. However, the absorption is not permanent because the color centers are unstable and eventually decay on their own. When the color centers

begin to decay, the displaced atoms in the silica lattice return to their intended location, and essentially reverse the damage done by the radiation. This decay of color centers decreases the absorption of the pump and signal wavelengths in the fiber and, therefore, increases the transmission. The reduction of absorption in the fiber is called recovery or annealing. Active recovery is the recovery experienced while the YDFL was on and lasing, while passive recovery is the recovery that occurred while the YDFL was off (dark).

The lifetimes for color centers vary depending on the type of defect that created them. At room temperature the color centers decay very slowly, while at high temperatures color centers decay (and recovery can occur) at a much faster rate. One study reported that an YDFA exposed to 100 krad(Si) of gamma radiation recovered back to its pre-irradiated power after being stored at room temperature for 2 years [34]. This suggests that all the color centers, for this specific dose, will decay on their own after a certain period of time. Fox et. al. reported that YDFs heated to 300°C for 8 hours recovered transmission of signals in the 1.0 - 1.7 $\mu$m range by 5 - 15% [17]. Another experiment concluded that heating an EDF to 450°C for 24 hours resulted in a recovery to 70% of its original (pre-irradiation) transmission [6].

# 3. Methodology

## 3.1 Overview

Previously published work focused on active Er or Yb fiber amplifiers, and damage done to fibers while dark, and then activated after irradiation to characterize the damage [2, 6, 10, 11, 17, 19]. This is the only work to date that analyzed the power output of an active YDFL while irradiated with gamma, and mixed gamma/neutron radiation. These experiments were setup to examine how the total radiation dose affected the power output of an YDFL with power measurements taken *in-situ*.

Irradiation from two different types of radiation sources were used in the experiments presented in this thesis. Gamma only irradiation from a $^{60}$Co source and mixed gamma/neutron irradiation from a reactor (the OSURR). For both sources the experiment was set up the same. A 1 meter length of pristine (never been irradiated) YDF was connected to the YDFL which acted as the gain medium of the laser. Then the YDF was irradiated while the YDFL was actively lasing. The power output of the YDFL was monitored *in-situ* as the total dose the YDF received increased over time.

## 3.2 Equipment and Materials Used

All of the equipment employed for the experiments conducted in this thesis was commercially available standard optical equipment. Table 1 lists each component that was used in the experiments. Before the experiments commenced, each component was thoroughly characterized by noting the loss, in dB, experienced as the components were added to construct the ring laser. Additionally, before each irradiation experiment, the performance of the YDFL was optimized for a power

output of roughly 20 mW.

**Table 1. Equipment used in experiments for this thesis.**

| Item | Specification |
|---|---|
| Yb-doped fiber for $^{60}$Co experiments | Liekki YB1200-6/125DC direct from manufacturer |
| Yb-doped fiber for reactor experiments | Liekki YB1200-6/125DC ordered from Thorlabs |
| 980 nm diode laser | JDSU S30-GPX57 |
| Bench top laser diode/TEC controller | SRS LDC501 ($^{60}$Co) |
| | Newport 6100 (reactor) |
| Butterfly mount | Newport 744 |
| Passive single mode fiber | Thorlabs P3-980A-FC-5 |
| Fiber optic isolator | Thorlabs IO-H-1064B-APC |
| Thor Labs output couplers | TW1064R3A2B (75/25 ratio) |
| | FC11064-50B-APC-1 (50/50 ratio) |
| | FC1064-99B-APC-1 (99/1 ratio) |
| WDM | WD202E-APC (980/1060 nm) |
| Optical Spectrum Analyzer | Yokogawa AQ6370 |
| Thorlabs power meters | PM100USB |
| | PM100D |
| Thorlabs power sensors (photodiodes) | S144C |
| | S155C |

### 3.3 Fiber Preparation

Fiber optics operate by guiding light through the core of the fiber. When one fiber must connect to another fiber, it must be done with great care. If not, significant loss may occur, and the signal through the original fiber may not couple into the second fiber (fully or at all). For the experimental setup for the YDFL in this thesis, there are two connection types that were exploited: fusion splicing, and ferrule couplers (FC). Fusion splicing uses a special instrument which aligns the two

ends of the fibers, then uses intense heat to join the two ends of the fibers together. This is the best type method of connecting two different fibers together, however, the splice is very brittle and can come apart quite easily. Also, this is a permanent connection, so it was not logical to use for every situation. For example, the YDFs for these experiments were switched out after each irradiation. Hence, permanent connection of the YDF to the YDFL was impractical. Instead the FCs were used to perform quick and easy connections/disconnections where practical or when the fibers came from the manufacturer with FCs already attached. While the FC/APCs are convenient to use, they do suffer more loss than fusion splicing, typically 3 dB per coupler used.

The optimum YDF length for the highest power output of the YDFL was modeled from the Fiber Amplifier and Laser Toolbox MATLAB program [35] by inputting the parameters of the measured losses from within the fiber ring laser and pump powers. The optimal length calculated was 1 m. The program was also utilized to determine the best input/output coupler ratio in the ring laser, which was 80/20. However, the only readily available output coupler at the 1060 nm wavelength was one with a 75/25 ratio. This slight change in ratio, according to the MATLAB fiber program, would incur a 7 mW reduction in power of the YDFL. This small power reduction was acceptable since maximizing power of the YDFL was not the focus of this thesis. As long as there was sufficient output power from the YDFL to monitor as it degraded from radiation damage then the experiments herein could be conducted.

The power of the pump laser was achieved by setting the current on the laser diode controller to 650 mA, and the to temperature 22 °C. The power output of the YDFL was monitored and recorded for 20 minutes prior to the start of experimentation to ensure stability. The loss from each FC/APC connector was

evaluated at the pump wavelength and recorded in Table 2 to aid in the modeling of the power output with respect to total radiation dose. The loss measurements were accomplished by connecting each component in succession to the previous component, starting from the pump laser and measuring the output of the components with the optical spectrum analyzer (OSA).

**Table 2. Measured loss from cavity components.**

| Location | Loss (dBm) |
|---|---|
| Pump laser through WDM | 1.5 |
| 99/1 output coupler | 1.6 |
| 5 m passive fibers (×2) | 2.5 each |
| YDF to passive fiber | 19.2 |
| 75/25 output coupler | 4.3 |
| Optical isolator to pump coupler signal | 2.0 gain |

### 3.4 Laser Characterization and YDFL Operation

The construction of the YDFL can be seen in Figure 6. The YDF is pumped with a 980 nm fiber coupled diode laser with a power output of about 300 mW. The laser was characterized by adjusting the current for the laser diode from a minimum of 50 mA to a maximum of 650 mA. The temperature for the diode was kept stable at 22 °C. The characterization of output power versus input current for the pump laser can be seen in Figure 7.

The pump laser was incorporated into the ring laser utilizing a WDM, which was then split into two paths using an output coupler. 1% of this light, from the ring laser, was siphoned off with a 99/1 output coupler. Then, this light was further divided in half with a 50/50 output coupler. This was done to allow dual monitoring of the pump laser and ring laser spectra with an OSA with one output, and a monitor to ensure the pump laser was still on and delivering power to the

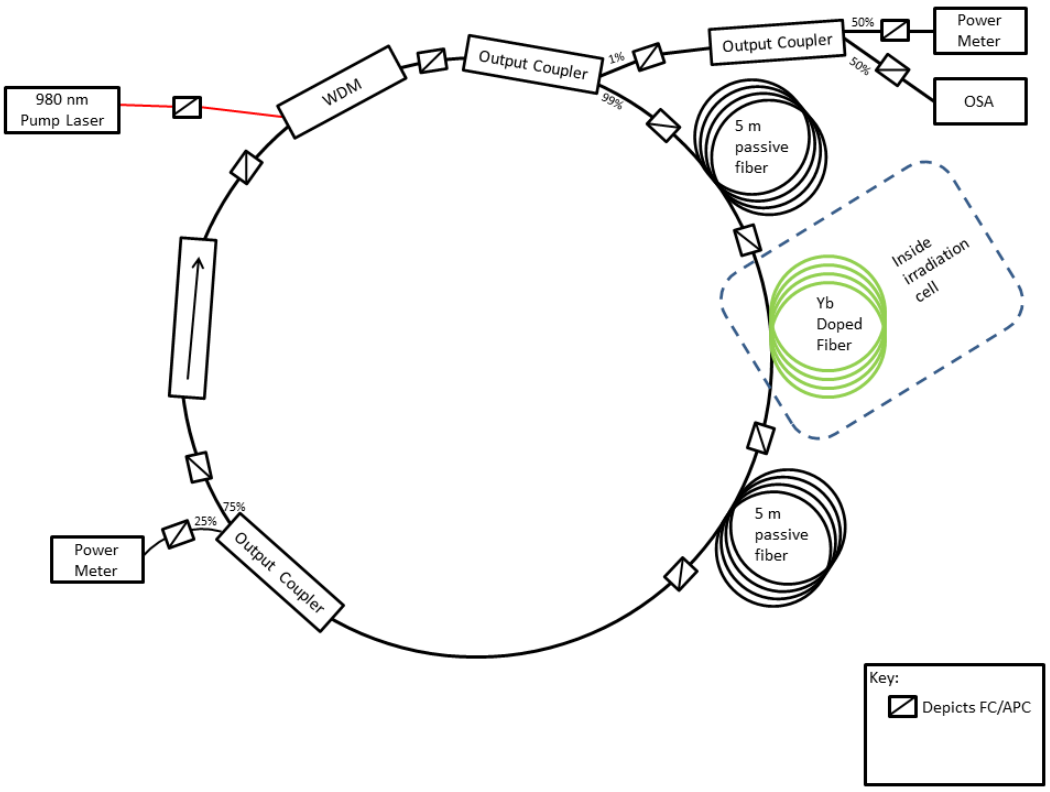


**Figure 6. Experimental setup for the ytterbium-doped fiber laser.**

YDF with the second output. The remaining 99% of the light traveled through 5 m of passive fiber to the YDF. Ideally, all of the pump signal would be absorbed within the YDF, and this was verified with OSA data taken during construction of the YDFL. The spectra for this configuration showed very little power at the pump wavelength of 975 nm after the pump signal propagated through the YDF. Next, an output coupler directs 25% of the laser's power to the power meter, while retaining 75% within the ring laser as feedback. Then the optical isolator restricts the 1064 nm signal, only propagating the light which is traveling in the clockwise direction (as shown in Figure 6), which keeps the laser operating within one mode [30]. The coherent light continues to travel clockwise within the ring and causing stimulated emission within the YDF until the radiation damage increases the attenuation in the YDF to a level that the pump lasers cannot sustain population inversion of the

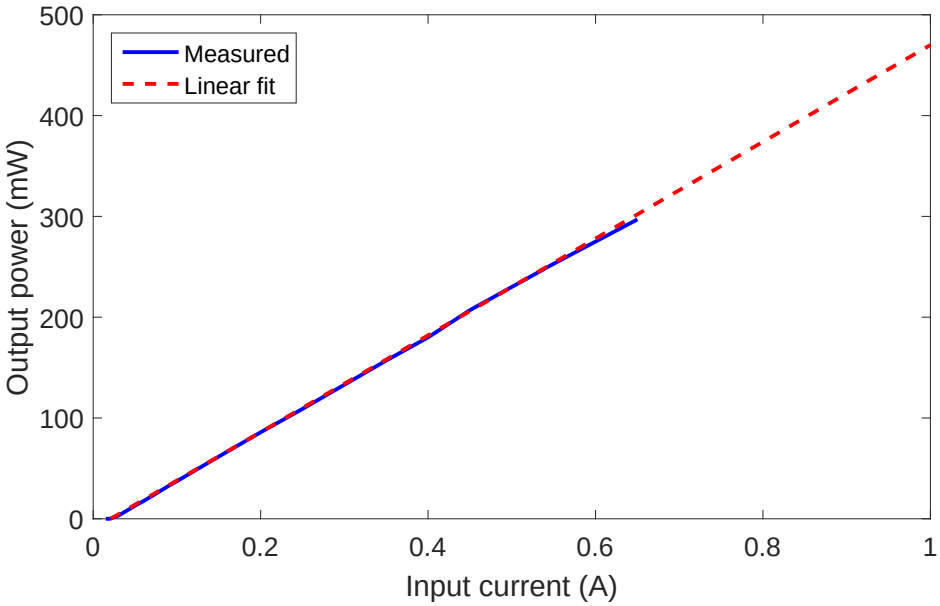


**Figure 7. Plot of input current versus output power for the laser diode (pump laser) measured with a power meter. The dashed line shows the expected power output for input currents larger than 650 mA.**

electrons in the ${}^2F_{5/2}$ energy level.

To determine the total RIA induced by irradiation the following steps were made. First, the initial power output of the YDFL was measured with a power meter from the 25% output of the output coupler. This measurement was taken just as the irradiation experiments began and is labeled as the initial power of the YDFL, $\mathrm{P}_{In}$. As the YDFL was irradiated, the output power of the YDFL, $\mathrm{P}_{Out}$ , was measured *in-situ*. The RIA is found using the formula for decibel loss per length given by

$$RIA(\lambda, t) = -\frac{10}{L_{YDF}} \times log_{10}\left(\frac{P_{Out}}{P_{In}}\right)(dB/m), \tag{3}$$

where $L_{YDF}$ is the length of the YDF and the minus sign simply denotes that the signal has decreased.

## 3.5 Irradiation Experimental Setups

### 3.5.1 Gamma Radiation Experiments

The $^{60}$Co irradiator cell at OSU sits at the bottom of a pool of water roughly 20 feet deep. A dry tube, 6 inches in diameter, was installed vertically and adjacent to the gamma cell. This allowed for experiments to be set up above the pool and affixed to an apparatus. Once ready, the apparatus (henceforth called the elevator) was lowered into place next to the gamma cell. The elevator was mechanically lowered from above the pool by a small crane. Specifically for the experiments here, the YDF in the YDFL had 5 m of passive fiber connected to it on each side. This allowed for the YDF to be placed in the dry tube and lowered to the gamma source while keeping the remainder of the YDFL at the top of the pool and away from any damaging radiation. Once the YDF was coiled up and situated on the elevator, the YDFL was turned on and characterized to ensure everything was working properly. Then, the YDF was lowered into the pool to a predetermined depth. The depth within the pool determined the dose rate the YDF experienced, with a maximum dose rate of 32.7 krad(Si)/hr. Once in place the YDF remained there, while the YDFL was actively lasing, for 4.5 hours, the time it took to reach the desired total dose of 150 krad(Si). After each experiment was conducted, the YDF was replaced with pristine YDF and then the experiment was repeated. Three $^{60}$Co experiments were conducted with this setup, but, due to a shortage of available YDF, the third experiment had to be altered. Therefore, the second experiment's YDF (YDF2) was re-irradiated for the final $^{60}$Co experiment. This fiber was exposed to a second dose of gammas for an additional 3.25 hours, at which time the YDFL no longer showed a signal at the 1060 nm wavelength.

### 3.5.2 Gamma/Neutron Radiation Experiments

The OSURR is a pool-type reactor composed of multiple dry tubes, beam ports, and a graphite thermal column (TC). The maximum operating power is 450 kW which, at this power, can achieve a maximum neutron thermal flux of $1\times10^{10}$ neutrons/cm$^2$/s in the TC. Once in place, the reactor was turned on and the YDF was exposed to continuous gamma/neutron irradiation while actively lasing. The OSURR experiments consisted of placing the YDF 10.16 cm inside the G7 position in the thermal column, which sits adjacent to the reactor's core. The thermal column is roughly 0.93 m away from the reactors core, with a 10 cm lead wall and an 82.9 cm wall of graphite bricks, called stringers, between the core and where the YDF was placed. The cavity where the YDF was placed was created by removing two of these stringers to create a small void in the TC. The reactor was operated at a greatly reduced power in order to extend the time the YDF was exposed to the neutron flux so measurements could be taken, and the degradation to the output power could be monitored. The reactor was operated at 50 W, 0.01% of the maximum power output, in order to achieve a reduced neutron flux of 1 $\times10^5$ neutron/cm$^2$/s. Subsequently, the reactor was run for 2.5 - 3.0 hours at powers ranging from 50 W - 450 kW. The maximum power of the reactor is 500 kW, however, OSU only runs it up to 450 kW to ensure they do not exceed the 500 kW power level they are regulated to never exceed. When the time objective was made for the day, the reactor as shut down and recovery data was taken for about 30 minutes. Then, as with the $^{60}$Co irradiator cell experiments, a pristine YDF replaced the irradiated YDF in the YDFL and a second experiment was conducted with the exact setup, but with the reactor at full power. Finally, a third experiment was conducted with the same setup as the previous experiment; however, the YDF was placed deeper in the TC, and the YDF from reactor experiment #2 was

re-irradiated in this experiment.

### 3.6 Active Recovery (Annealing) Experiments

Active recovery experiments were conducted following irradiation from a radiation source (either from the gamma only source or the mixed gamma/neutron source). Regardless of which radiation source was used, the procedure for the active recovery experiments was identical. The YDFL would remain on, and the power and spectra of the YDFL were monitored in the same manner as the irradiation experiments. Then, the YDFL would remain in place, and a second recovery experiment was conducted 18 - 30 hours later. After the second active recovery experiment, the YDF would be removed from the YDFL to allow for more irradiation experiments to be conducted. Finally, the YDFL was moved to the lab where three more recovery experiments were conducted on the YDFs irradiated with gamma only radiation. The reason for discontinuing the active recovery experiments on the YDFs irradiated by the mixed neutron/gamma source will be discussed later.

### 3.7 Uncertainty and Error Propagation

The confidence of the measurements taken herein must be discussed to ensure accuracy. In this section the equipment used to record the power measurements will be discussed, and the accuracy and uncertainty of the measurements will be analyzed. Uncertainty that is carried forward in calculations is called propagation of error, and must also be explored in order to ensure the results presented in this thesis are accurately represented [36].

The power measurements presented in this thesis were recorded using the Thorlabs PM100D power meter which was connected to a laptop via a USB cable. The laptop was installed with the Thorlabs PM100/PM200 software which allowed

the power measurements to be recorded digitally. This software utilized the LabVIEW 8.5.1 software and drivers distributed by National Instruments. The power meter software on the laptop allowed for the frequency of the data collection to be varied. For all experiments the frequency was set to 0.5 Hz (measurements taken every 2 seconds).

The power sensor used in conjunction with the power meter was the Thorlabs S144C with a fiber optic connector. This connector allowed for the power output from the YDFL (the 25% output from the 75/25 output coupler) to be screwed onto the power sensor for more accurate readings. The range of power that this sensor could be used for was 1 $\mu$W - 500 mW. The range of power measurements taken in the experiments, approximately 45$\mu$W - 30 mW, fell within the reported range of the sensor. The uncertainty of the measurements must now be explored.

The uncertainty in the power measurements recorded using the power sensor was reported by the manufacturer as $\pm$ 5%. This will have a varied effect as the power of the YDFL increases or decreases. For initial power readings at the start of the experiments, the power of the YDFL was usually around 25 mW. For readings in 10 - 25 mW range, the maximum uncertainty would be $\pm$ 1 mW. This implies that the range of an initial power reading would be 25 mW $\pm$ 1 mW. As the power reading decreases, so too will the uncertainty. If a power reading is in the 25 - 40 $\mu$W range, the maximum uncertainty would be $\pm$ 2$\mu$W. This would give a possible final power reading of 40$\mu$W $\pm$ 2$\mu$W. These two examples encompass the range of minimum and maximum values of YDFL power that was seen in the irradiation experiments presented in this thesis.

However, the power meter measured the power of the YDFL more precisely than the manufacturer reported, evidenced by the data which indicated stability in the power measurements up to the 10 $\mu W$ place. The 1 $\mu W$ place fluctuated up to

$\pm 8\,\mu W$. For this reason, a more accurate estimate of uncertainty in the power meter of $\pm 10\,\mu W$ will be employed, rather than using the general estimate of uncertainty reported by the manufacturer.

Another area for uncertainty involves the measurement and cutting of the YDF to a length of 1 m. The measurements were made using a tape measure with millimeter increments. Therefore, the uncertainty of the length measurements, $dL$, would be $\pm$ 0.001 m and the best estimate for the length, $L_{best}$, would be 1.000 m [36]. Therefore, the measured value of the length of the YDF, $L$, would be

$$L = L_{best} \pm \delta L = 1.000 \pm 0.001\,[m]$$

The only instance in which the power data and the length of the YDF were used to calculate another value was for the determination of RIA. This calculation is a simple logarithmic scaling of the ratio of measured powers at a given time versus the initial power. According to Taylor, any propagation error problem can be solved using equation 4 [36].

$$\delta q = \left[ \left( \frac{\partial q}{\partial x} \delta x \right)^2 + \left( \frac{\partial q}{\partial y} \delta y \right)^2 + \left( \frac{\partial q}{\partial L} \delta L \right) \right]^{1/2} \tag{4}$$

This equation has been adjusted to reflect the number of separate measurements present in this thesis. Specifically, $x$ and $y$ are the measured power of the YDFL taken from the power meter, $L$ is the measured length of the YDF, and $\delta x$, $\delta y$, and $\delta L$ are the uncertainties of their respective measurements. These values are used to calculate the function $q(x, y, L)$, which is the RIA calculation in equation 3; however $y$ now represents $P_{out}$ (the measured power at a certain time after irradiation was initiated), and $x$ represents $P_{in}$ (the measured power prior to irradiation).

Next, the partial derivative of the RIA was found for each of the three variables

in the function. The partial derivative of $q$ with respect to $x$ is

$$\frac{\partial q}{\partial x} = \frac{10}{L \cdot x \cdot \ln(10)}$$

The other two partial derivatives were calculated in the same way, and are not shown. Then, the measured values of $x$, $y$, and $L$, along with the values of uncertainties discussed above were plugged into the three equations produced from the partial derivatives of the RIA equation. In this example, the measured values of $x$, $y$, and $L$ were 25 mW, 40 $\mu$W, and 1 m respectively. With the equation 4, the total uncertainty in the RIA calculation, becomes

$$\delta q = \left[\left(173.7178 \cdot 10^{-6}\right)^2 + \left(-108,570 \cdot 10^{-6}\right)^2 + \left(-27.9588 \cdot 0.001\right)\right]^{1/2} = 0.1477$$

The RIA calculation for this case, with uncertainty considered is

$$RIA = -\frac{10}{L} \times log_{10}(\frac{y}{x}) = 27.9588 \ \pm \ 0.1477 \, (dB/m)$$

The propagation of error for the case explained above had the largest difference regarding the ratio of power measured before and during irradiation. Furthermore, this case had the largest percentage of error for the data presented in this thesis. The error was $\pm$ 0.5284% in RIA. Further calculations were run with measured power values closer to the initial power measurement of 25 mW; these calculations demonstrated a much lower error of RIA. For a measured power of 23 mW and an initial power measurement of 25 mW, the error in RIA was found to be less than 0.0003%.

# 4. Results of Gamma Irradiation on an YDFL

## 4.1 Chapter Overview

The gain medium (YDFs) in an YDFL were irradiated with a $^{60}$Co gamma source while actively lasing. The power of the YDFL was monitored *in-situ*, and spectra of the pump laser and signal created by the YDFL were collected. The first two experiments were conducted on YDF1 and YDF2 respectively. Each was exposed to the gamma irradiation cell for 4.5 hours, receiving total doses of 145 krad(Si). For the third experiment, YDF2 was exposed to an additional 100 krad(Si) dose of gamma radiation. Following each experiment, the YDFs were kept in place on the elevator, and the YDFL continued lasing for varied lengths of time (depending on the OSURR schedule). The purpose of the recovery data collected was to investigate if the radiation damage could be annealed (repaired) at room temperature with the YDFL actively lasing (active recovery). The annealing would be proven possible if the power showed a significant increase over a relatively short time frame (a maximum of 12 consecutive hours). Annealing would also be investigated in the YDFs when the YDFL was turned off for many hours then turned back on a day or two later (passive recovery).

It has been shown previously that the damage mechanism that plays the biggest role in optical fibers is the creation of color centers within the fiber [2]. These color centers can absorb the pump signal and/or the lasing signal which adversely affect the power of the YDFL. In other studies, it has been seen that the most radiation susceptible component of a rare-earth doped fiber laser is the RE-doped fiber itself [12]. Hence, the experiments within this thesis limit the exposure of radiation to the YDFs, the gain medium of the YDFL built for these experiments.

## 4.2 Experiment

### 4.2.1 Irradiation Source Description

The gamma source used for these experiments was a pool-type $^{60}$Co gamma cell. The gamma source itself was a cylindrical slab of cobalt which sat at the bottom of a 15' deep pool of water (roughly 25' ×25'×15'). In order to access the gamma source, a 6" dry tube was placed adjacent to the cobalt which extends upwards to the top of the pool. A mechanical lift held a platform to which samples could be placed on or attached to. This is referred to as the elevator. The elevator allowed the sample to be lowered into the tube to place the sample at a certain height above the gamma source. The height in the tube determined the dose rate the sample experiences. The maximum dose rate, 32.3 krad/hr, was achieved at a height of 8 inches from the bottom of the pool.

### 4.2.2 Experimental Setup

The YDFL was setup on the top of the pool which housed the $^{60}$Co gamma cell. The YDF was spooled up (3 loops with a 2" diameter) and taped down to the bottom of the dry tube elevator. Two 5 m long patch cables were connected to both ends of the YDF, and were routed upwards to the top of the dry tube elevator. The patch cables were also taped into place to restrict movement of the fibers, and to keep them contained so that the elevator could be lowered into place. The YDFL was then turned on, and initial spectrum and power measurements were taken. The laser diode controller/TEC was set to 650 mA of current and to a temperature of 22° C. The YDFL was allowed to run for 20 minutes to ensure the power level was stable. Once this time had elapsed, the elevator was lowered into position to the peak irradiation location of 8 inches from the bottom of the pool. This process took about 20 seconds. At this location the dose rate was 32.3 krad/hr. The YDF was

kept in place for a total of 4.5 hours, until the total dose accumulated was 145 krad(Si). This experiment setup was used for both YDF1 and YDF2. Once the desired total dose was achieved, the elevator was raised and the YDFL was kept running for a period of time in order to record recovery data. Once the recovery data was recorded, the laser was powered off, and the YDF was removed from the elevator and disconnected from the YDFL. The YDF, YDFL, and instrumentation placement was consistent for each experiment with the exceptions of replacing the YDFs between each experiment, and lowering the YDFs into the gamma cell (the 5 m passive cables would move).

The third experiment using the $^{60}$Co gamma cell was setup exactly as the first two experiments. The only difference was the YDF used was not a pristine fiber, but a fiber that was already exposed to a dose of 145 krad(Si) in the second experiment (YDF2). The YDFL was turned on and recovery data was taken for an hour. Then, the elevator was lowered to bring the YDF into position next to the gamma source. For this third experiment, the YDF was kept in the gamma irradiation cell until the laser's power had degraded to the point which the wavelength of the YDFL (1060 nm) could no longer be seen on the OSA. This occurred at 3.25 hours into the experiment, resulting in YDF2 receiving a total accumulated dose of 252 krad(Si). The fiber was then raised out of the pool and kept in place on the elevator for 2 hours. The laser remained on and initial recovery data was taken over this period of time. After the initial recovery data was collected, the laser was shut off and the YDF was removed from the elevator and disconnected from the YDFL.

### 4.3 Results and Discussion

Degradation of the power of the YDFL was measured *in-situ* to determine vulnerability of the YDF, since these fibers have been shown to be the most

radiation susceptible part of the YDFL. Also, the spectrum for the YDFL was monitored in order to determine how the radiation damage would affect the spectrum of the laser. Previous studies have reported shifts in the lasing spectral regions of the RE-doped fiber lasers from effects induced by radiation damage. The reported causes of the laser spectrum shifts were effects from color centers, thermal effects, and changes to the optical cavity length [19].

### 4.3.1 YDF1

#### 4.3.1.1 Irradiation

The power degradation in the YDFL started immediately after the fiber was lowered into the gamma irradiation chamber and continued until the fiber was raised out of the chamber. The power degradation experienced by YDF1 can be seen in Figure 8, which clearly shows an exponential loss in power as the dose increases linearly with time. After exposing YDF1 to a total dose of 145 krad(Si), its power decreased from 22 mW to 416 $\mu$W. Using the initial power reading for the YDFL, just prior to irradiation, the loss in power per unit length (dB/m) was calculated as 17.1 dB/m and can be seen plotted with respect to total dose in Figure 9. The spectrum for the YDFL with YDF1 used as the gain medium was measured before, during, and after the irradiation. The lasing spectrum prior to irradiation indicated a fairly broad range, from 1046 - 1058 nm. The lasing spectrum began to shift toward shorter wavelengths and began to sharpen as exposure to gammas occurred. This shift is shown in Figure 10. The final measured lasing wavelength after a dose of 145 krad(Si) was 1039 nm with a peak width of roughly 1 nm.

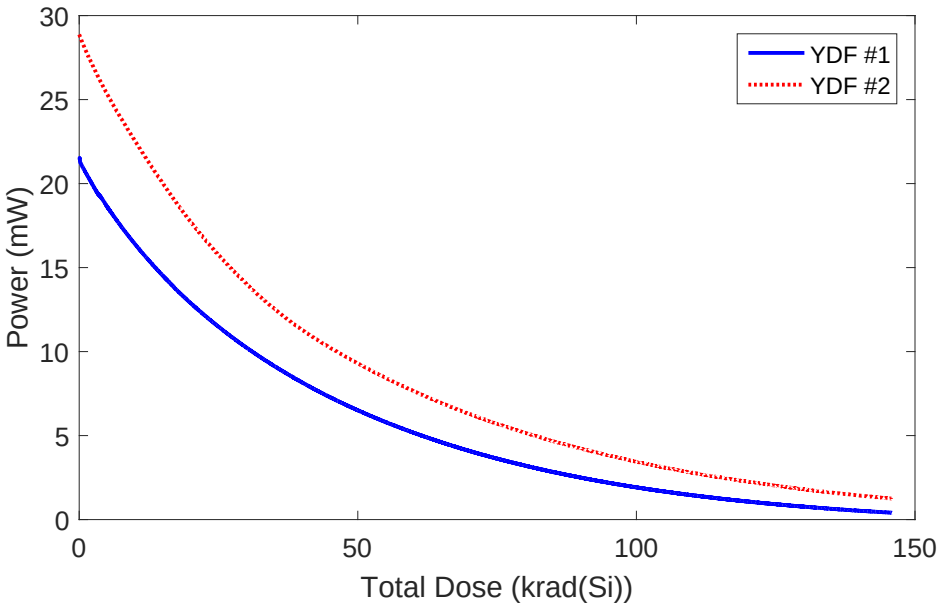


**Figure 8. An exponential decrease in power was seen for both YDFs as the dose increased from 0 to 145 krad(Si) over the course of 4.5 hours.**

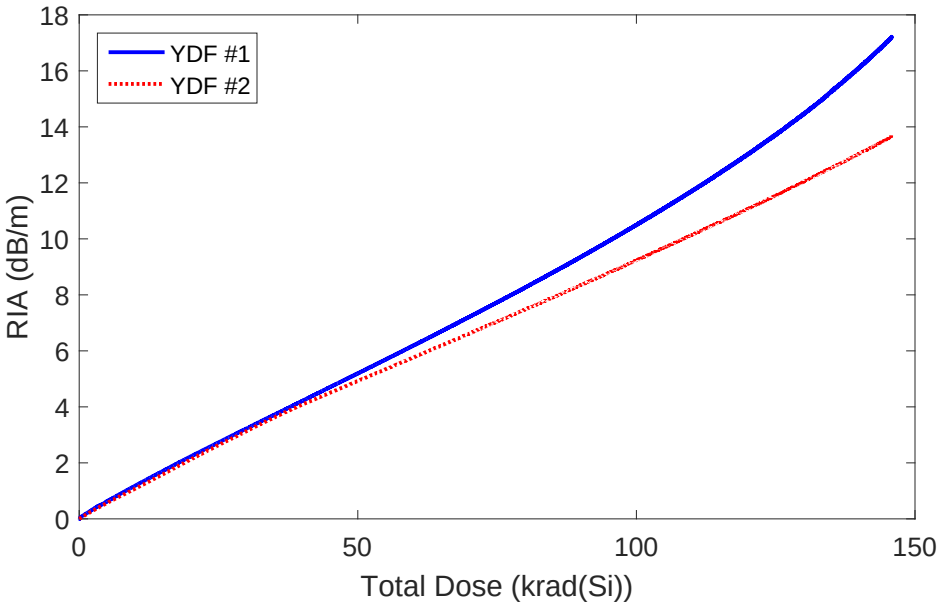


**Figure 9. The RIA for both YDF1 and YDF2 increases linearly as the total dose increases over time.**

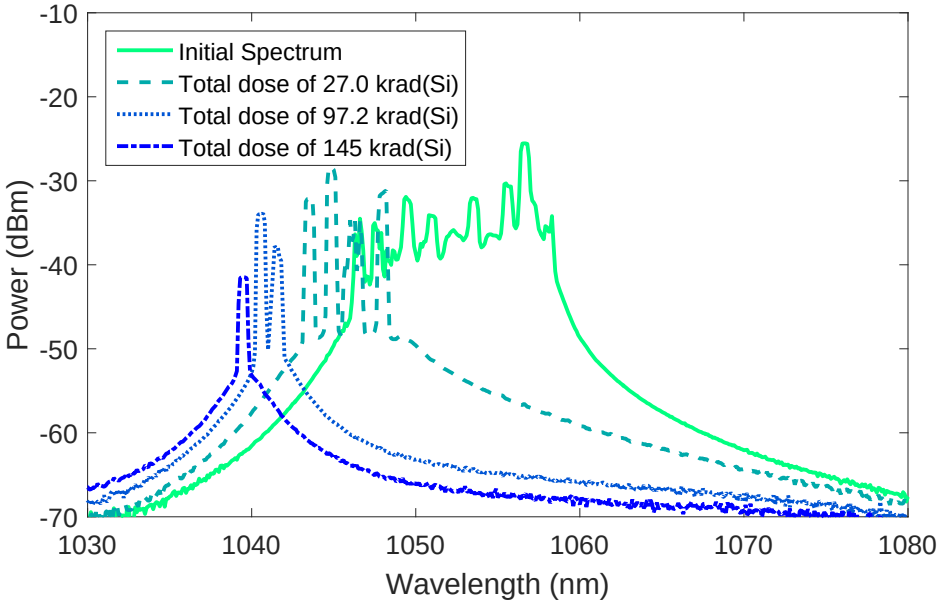


**Figure 10. The lasing wavelength for the YDFL with YDF1 as the gain medium. The lasing wavelength shifted to shorter wavelengths as the total gamma dose increased.**

#### 4.3.1.2 Damage Recovery

Immediately following the irradiation of YDF1, active recovery data was taken for 1 hour. The power of the YDFL increased a total of 266 $\mu$W from its post irradiation power of 416 $\mu$W to 682 $\mu$W. The YDFL was then shut off and the fiber was left in place on the elevator overnight. The following morning, 18 hours after YDF1 was irradiated, the YDFL was turned back on and the fiber experienced an increase in power of 97 $\mu$W from passive recovery overnight. The laser remained on for another 20 minutes, and the active power recovery was monitored again. During this time the laser power increased a total of 142 $\mu$W, from 797 $\mu$W to 939 $\mu$W. After 20 minutes of active recovery time, the YDFL increased its power 154% more in 0.02% of the time than it did passively for 18 hours. The YDF was then removed from the elevator and the YDFL in order to perform irradiation experiments on another fiber. All subsequent recovery data for this fiber was performed in the lab.

The initial power reading upon reconnecting YDF1 to the YDFL in the lab was

higher than the final power reading recorded at OSU. The YDF and passive fibers were disconnected at OSU, moved back to the lab, and then reconnected in the lab for further measurements. Because the fibers were relocated, it is difficult to determine if the power gain occurred due to passive recovery or from a difference in how the fibers were configured. Simply touching or moving any of the fibers of the YDFL caused fluctuation in the power of the laser. This was seen during experiment setups, elevator movement, and accidental bumps of the fibers.

The third set of recovery data for YDF1 was taken at 90 hours post irradiation. At the commencement of this data collection, the YDFL power was 1.5 mW, up 561 $\mu$W from the last power reading of the second active recovery period. This shows that the YDF once again recovered from radiation damage without any light being transmitted through it. The laser was left on for about 13 hours and the YDFL was able to recover another 1.5 mW of power. The following day (at 118 hours post irradiation) the laser was turned on again. After sitting dark for another 16 hours the YDFL gained 68 $\mu$W of power. However, after about 12 minutes of the laser being on, the power decayed slightly for about 25 minutes before it began to increase in power again. After 5.5 hours of active recovery, the YDFL gained another 173 $\mu$W, reaching a final power level of 3.3 mW. Each of the active power recovery experiments can be seen in Figure 11. The slopes of these plots will be used in the analysis chapter to calculate the total time it would theoretically take the YDFL to recover to its pre-irradiation power level. In a published experiment by Mady et al., it was shown that transmission in irradiated fibers did not recover beyond 50% until the fibers were heated to 350 °C [21]. Therefore, actively recovering to full power at room temperature would not be expected from any of the experiments performed in this thesis.

The spectral data taken during the active recovery sessions for YDF1 can be

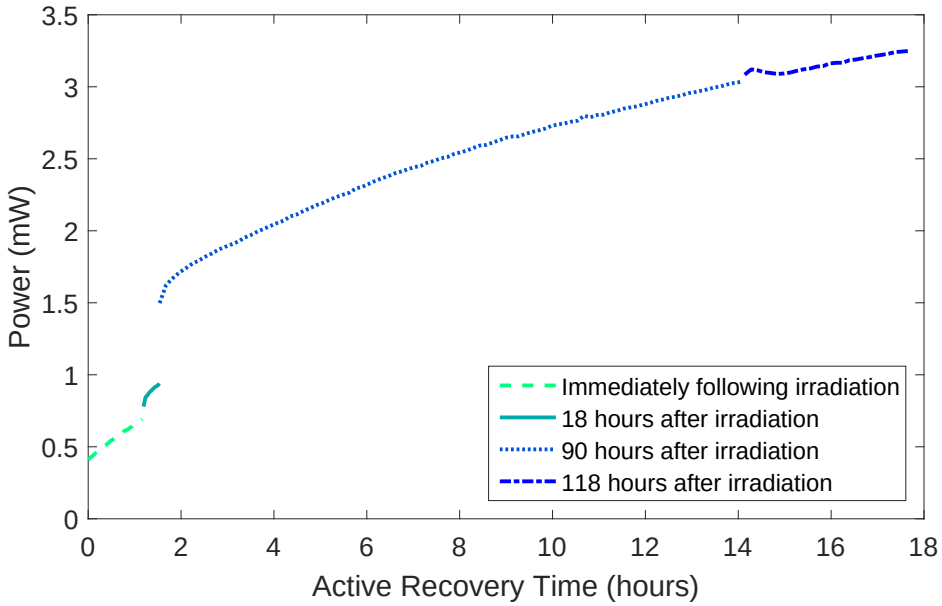


**Figure 11. The power for the YDFL increased at a higher rate of recovery immediately following irradiation of YDF1. The power recovered roughly 100 $\mu$W overnight while the fiber was dark. Then the laser was turned back on and the fiber recovered at roughly the same rate as before. After 90 hours of passive recovery, the active recovery rate for the fiber reduced significantly and remained constant for the remainder of active recovery.**

seen in Figure 12. The lasing wavelength of the YDFL redshifted from 1039 nm to 1041 nm over the course of 17.63 hours of total active recovery time. During this shift, the width of the peak broadened some, to roughly 1.5 nm in width during the transition to the longer wavelength. However, the spectrum narrowed back to its initial width of 1 nm just prior to the end of the active recovery experiment.

### 4.3.2 YDF2

#### 4.3.2.1 First Irradiation

The pre-irradiation power for the YDFL using YDF2 that was measured just prior to being lowered into the gamma irradiation chamber was 28 mW. Once lowered into the chamber the power of the YDFL began to decrease until it was removed from the irradiation chamber 4.5 hours later. Upon removal from the

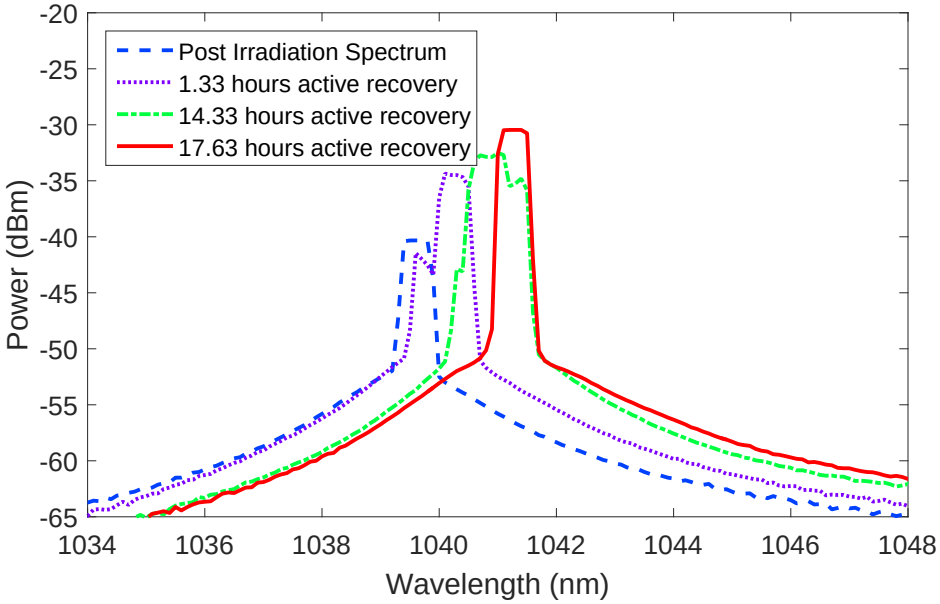


**Figure 12. The results for all power recovery spectral data taken for YDF1. The lasing wavelength redshifted a total of 2 nm during the active recovery experiment. The spectrum also showed a slight broadening of the peak during the transition to the 1041 nm peak wavelength. However, at the conclusion of the active recovery experiment, the width narrowed back to its initial width of 1 nm.**

irradiation chamber, the final power measured was 1.47 mW. The power reduction versus increasing gamma radiation dose can be seen in Figure 8. YDF2 followed a similar exponential power loss that was seen in the first experiment with YDF1. The total power loss of YDF2 calculated was 13.7 dB/m. RIA increased for YDF2 and YDF1 as the total gamma dose increased over time; this is shown in Figure 9. The power loss, measured in dB/m, in both fibers increased linearly as the dose increased roughly linearly with time. The spectral data, shown in Figure 13, also followed the general trend in data collected with YDF1. These results show the lasing wavelength shifted to shorter wavelengths (blueshift) as the gamma dose increased in the fiber. The lasing spectrum for YDF2 started out sharper than YDF1, with its peak at 1056 - 1058 nm. After 145 krad(Si) dose of gamma irradiation, the lasing wavelength shifted to 1039 nm with a sharpness of roughly 1 nm.

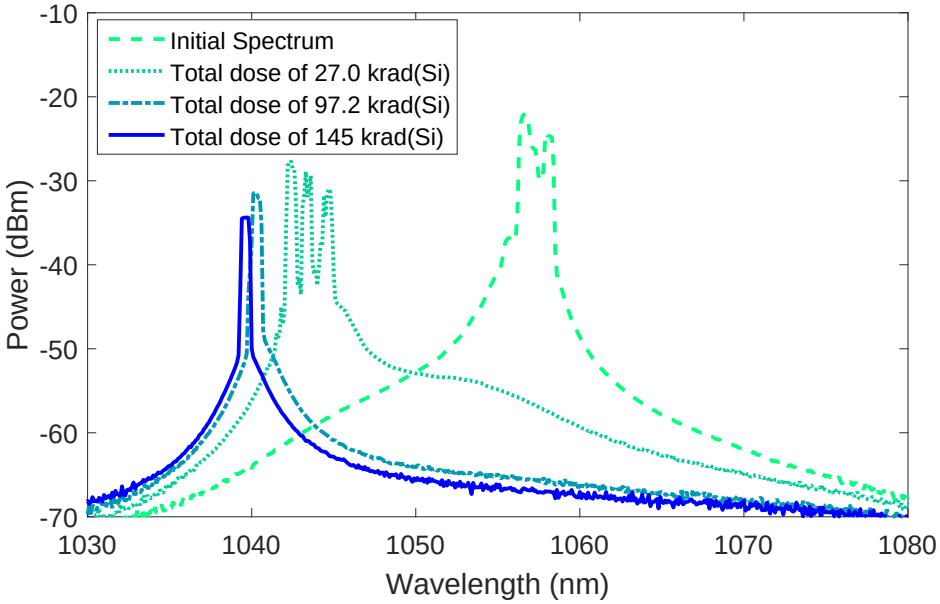


**Figure 13. The lasing wavelength for the YDFL with YDF2 in the ring cavity. The lasing wavelength shifted to shorter wavelengths as the total gamma irradiation dose increased. The total shift in wavelength was roughly an 18 nm blueshift.**

#### 4.3.2.2 First Damage Recovery

The YDFL began to increase in power with active recovery after YDF2 was raised out of the irradiation chamber. The power of the YDFL was 1.23 mW after the elevator was raised to the up position. This marked the starting power for the active recovery data for YDF2. The YDFL actively recovered for 1.7 hours and experienced an 850 $\mu$W power increase. The YDFL was then shut off and remained in the same position for two days. The morning of the second irradiation experiment (2 days later), the YDFL was turned back on and allowed to recover for an additional 1.5 hours. The starting power for the YDFL after its 40 hours of passive recovery was 2.08 mW, which was the same power level observed the last time it was on. This contradicts the first experiment where YDF1 increased in power by 68 $\mu$W after 18 hours of passive recovery. The possibilities as to why this happened will be discussed in the analysis chapter. After the 1.5 hours of active damage recovery the YDFL power was 2.59 mW, up 510 $\mu$W. The data for both active

power recovery sessions can be seen in Figure 14. The spectral data for YDF2 for a total dose of 145 krad(Si) indicated that the lasing wavelength redshifted 1 nm, from 1039 nm to 1040 nm, with a slight broadening of the peak at the conclusion of the second recovery time (labeled as "3.5 hours of recovery" in Figure 15).

#### 4.3.2.3 Second Irradiation

YDF2 was not moved since being placed on the elevator for its initial irradiation experiment. After its first irradiation experiment, the elevator was raised to remove YDF2 from the irradiation chamber and two sessions of active recovery data were collected. Then, keeping everything in place, the second and final $^{60}$Co gamma irradiation experiment on YDF2 commenced. For this final gamma re-irradiation experiment, YDF2 was exposed to an additional 107 krad(Si) dose of gamma radiation. The power of the YDFL was slightly lowered to 2.33 mW once YDF2 had been lowered into the $^{60}$Co chamber. Similar to the previous two experiments, the power of the YDFL began to immediately decay moments after the YDF was lowered into the irradiation chamber. YDF2 was left in the gamma cell for 3.25 hours, allowing the fiber to receive enough radiation damage to reduce the lasing signal of the YDFL into the noise level of the OSA, shown in Figure 16. Subsequently, since the YDFL was no longer lasing, it was removed from the irradiation chamber. During its total time in the gamma irradiation cell, from both experiments #2 and #3, YDF2 received a total gamma dose of 252 krad(Si). The total YDFL power loss from this final experiment was 2.3 mW, which also followed an exponential decay as seen in the previous two experiments. The power decay for experiment #3 can be seen in Figure 17, which also exhibits the power decay from the previous two experiments on YDF1 and YDF2. The total power loss for YDF2 in its second irradiation was 17.34 dB/m, evidenced in Figure 18. This was the

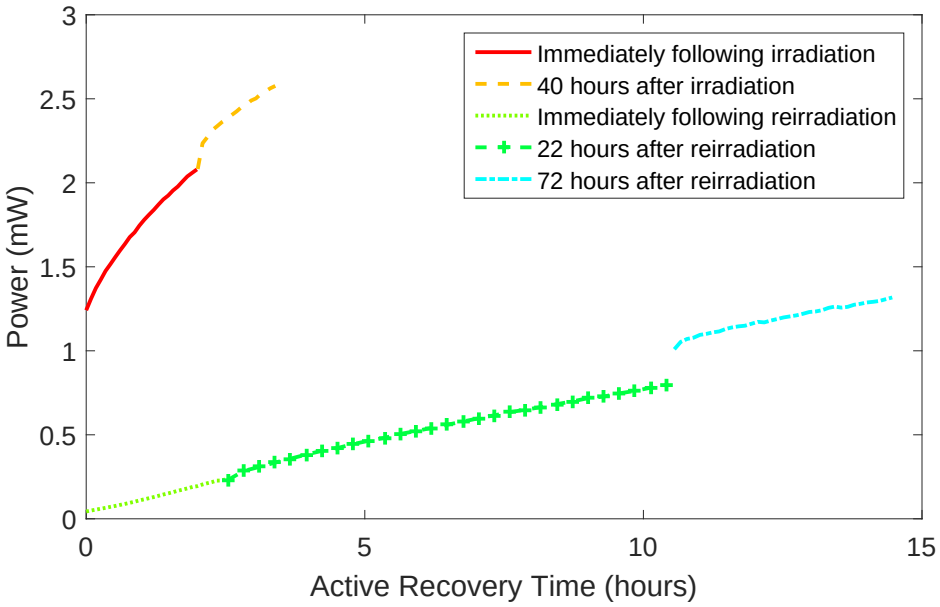


**Figure 14. The results for all power recovery data taken for YDF2. The power recovered the fastest after the first irradiation, with an average power recovery slope of 0.28 mW/hr. After being irradiated a second time, the average recovery slope for the final three recovery runs averaged 0.071 mW/hr. The greatest passive recovery was seen between the final two runs after YDF2 was re-irradiated. The power recovered 227 $\mu$W passively here, where all other passive recovery times for YDF2 did not yield any gain in power.**

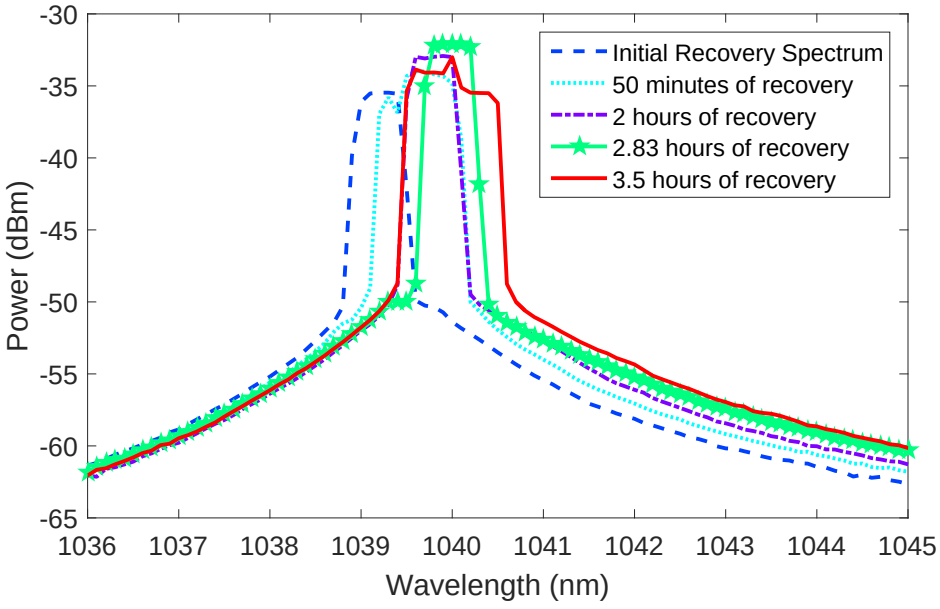


**Figure 15. The results for all power recovery spectral data taken for YDF2. The lasing wavelength redshifted a total of 1 nm during the active recovery experiment. The spectrum also showed a slight broadening of the peak, roughly 1.5 nm, at the conclusion of the active recovery time.**

highest power loss out of the three experiments with the shortest irradiation time.

The lasing wavelength of the YDFL blueshifted slightly once exposed to irradiation. The initial lasing wavelength for the YDFL was 1040 nm, and after a total dose of 228.7 krad(Si) shifted to 1038.5 nm. After receiving a total dose of 252 krad(Si) the signal at the lasing wavelength could no longer be distinguished above the noise level of the OSA. The total spectrum shift from a pristine YDF2 to a total gamma dose of 252 krad(Si) is shown in Figure 19.

#### 4.3.2.4 Second Damage Recovery

Once the lasing signal was no longer apparent in the OSA measurements, the elevator to the gamma irradiation cell was raised to allow YDF2 to recover. The fiber, as in the past two experiments, was allowed to recover while still attached to the elevator immediately following irradiation (labeled "re-irradiation" in Figure 14). YDF2 recovered for 2.25 hours where it experienced an increase in power of 195 $\mu$W. At the conclusion of this recovery period, the YDF was removed from the elevator. While removing YDF2 from the elevator, one of the spliced connector fibers broke off from the YDF. This connector fiber was spliced back onto YDF2 the next day in the lab. It should be noted that a small portion of the YDF and the connector fiber was cut away in order to have pristine cleaved ends to splice together. Therefore, any recovery data after the immediate recovery data for the re-irradiation experiment will be with an YDF and connector fiber that are both roughly 25 mm shorter. When YDF2 was connected back to the YDFL in the lab, the initial power reading was down 6 $\mu$W from the last power reading taken before the YDF was removed from the elevator. The power loss experienced here is assumed to be from the re-splicing of the connector fiber to the YDF. This power loss would make it difficult to determine if any passive power recovery occurred

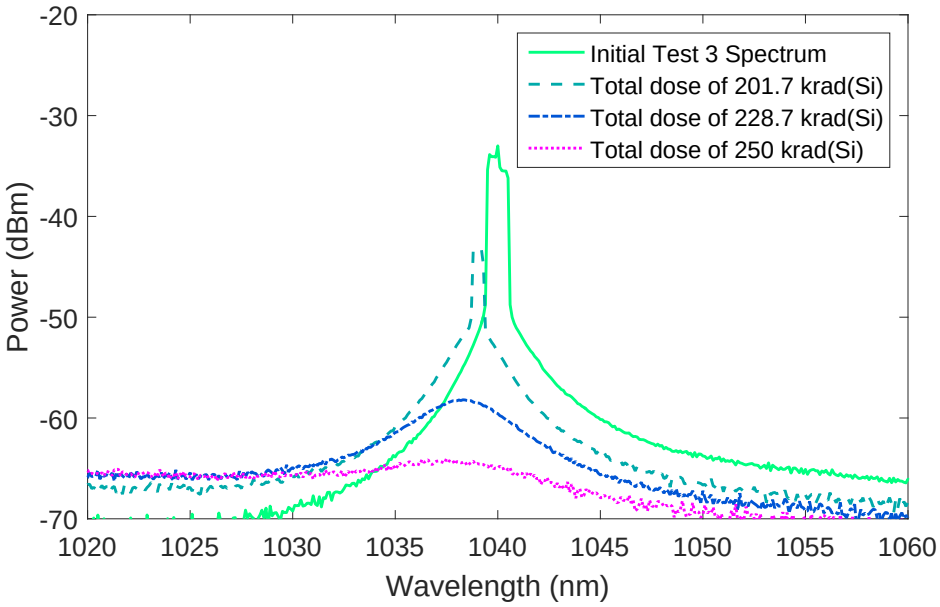


**Figure 16. The lasing wavelength for the YDFL with YDF2 in the ring cavity. The lasing wavelength shifted to shorter wavelengths as the total gamma irradiation dose increased. The total shift in wavelength was roughly a 1.5 nm blueshift until the power at that wavelength was practically zero.**

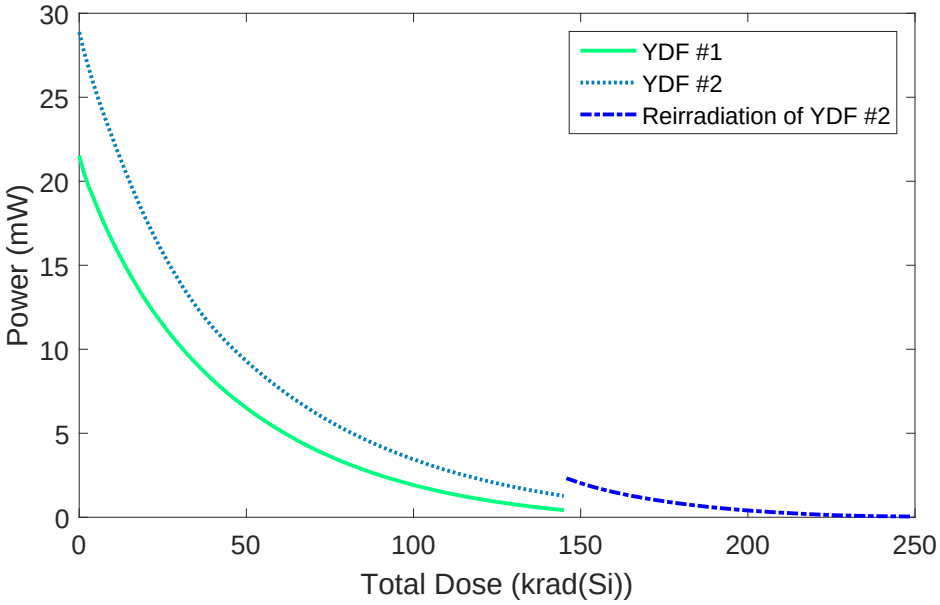


**Figure 17. This figure shows the exponential decay in power with increasing dose. The YDFL with YDF1 had a starting power of 22 mW which degraded to 416 $\mu$W after a total dose of 145 krad(Si). The initial power for the YDFL employing YDF2 was 29 mW, and decreased exponentially to 1.47 mW after a 145 krad(Si) dose. After actively recovering for 3.2 hours and passively recovering for 16 hours, YDF2 was irradiated again. The starting power for its second irradiation was 2.3 mW and degraded exponentially to 45 $\mu$W after a total dose of 252 krad(Si).**

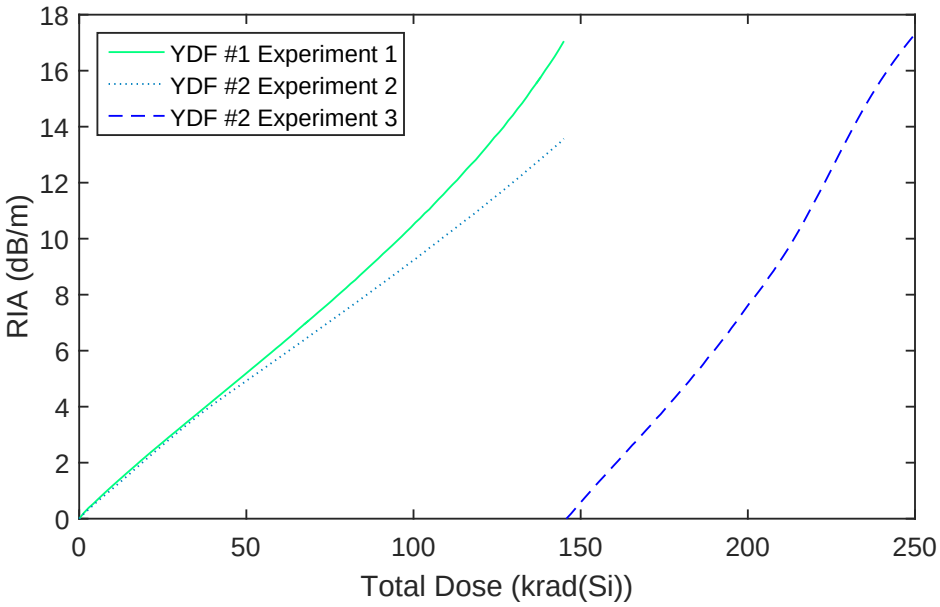


**Figure 18. The total power loss for both YDF1 and YDF2. The power loss for each fiber increased linearly with increasing gamma dose.**

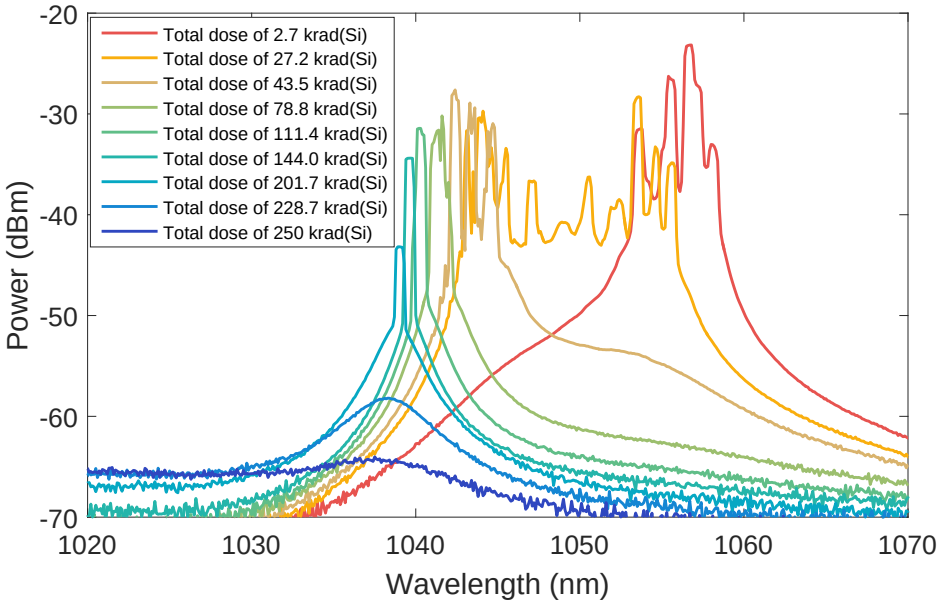


**Figure 19. The lasing wavelength can be seen to shift toward the blue side of the spectrum with increasing gamma dose. The spectrum broadened to almost 20 nm after a dose of 43.5 krad(Si), but then began to sharpen after receiving a dose of 78 krad(Si). Once the total dose approached 250 krad(Si), the lasing wavelength was barely visible on the OSA.**

since the length of the YDF was shortened slightly.

The YDFL was setup in the lab, 22 hours post re-irradiation, and YDF2 was connected to the ring cavity and actively recovered for 8 hours. During this time, the power increased a total of 573 $\mu$W, up to 803 $\mu$W from 230 $\mu$W. The YDF was disconnected once more from the YDFL in order to record recovery data for YDF1. The following day, YDF2 was reconnected to the YDFL and actively recovered for four more hours. Once connected, the initial power of the YDFL was higher than the previous day. It had passively recovered 227 $\mu$W of power, almost half of its active power recovery from the day prior, in roughly 19 hours. For the final four hours of active recovery, YDF2 increased in power another 290 $\mu$W, leaving the final recorded power at 1.32 mW.

Figure 20 shows that the sharp and narrow peak typical of a laser was no longer seen at the start of recovery. The radiation damage suffered by YDF2 was detrimental enough to prevent the laser from lasing. As the damage recovery began, the power at the lasing wavelength started to rise, but was quite broad. While the spectrum for the lasing signal was broad, a slight redshift could still be seen as the signal began to recover power. A narrow lasing peak could not be distinguished until the 2.5 hour point in the recovery experiment. From the time period of 2.5 hours to 6.5 hours, the peak rose in power and redshifted roughly 0.75 nm to 1039 nm. After this shift at 6.5 hours, no more shifts in lasing wavelength were seen for the remainder of the active recovery experiment.

### 4.4 Summary

The power degradation of the YDFL was measured *in-situ* while, in-turn, two YDFs were exposed to gamma irradiation from a $^{60}$Co source housed at OSU. Each of the YDFs were separately installed as the gain medium for the YDFL, and were

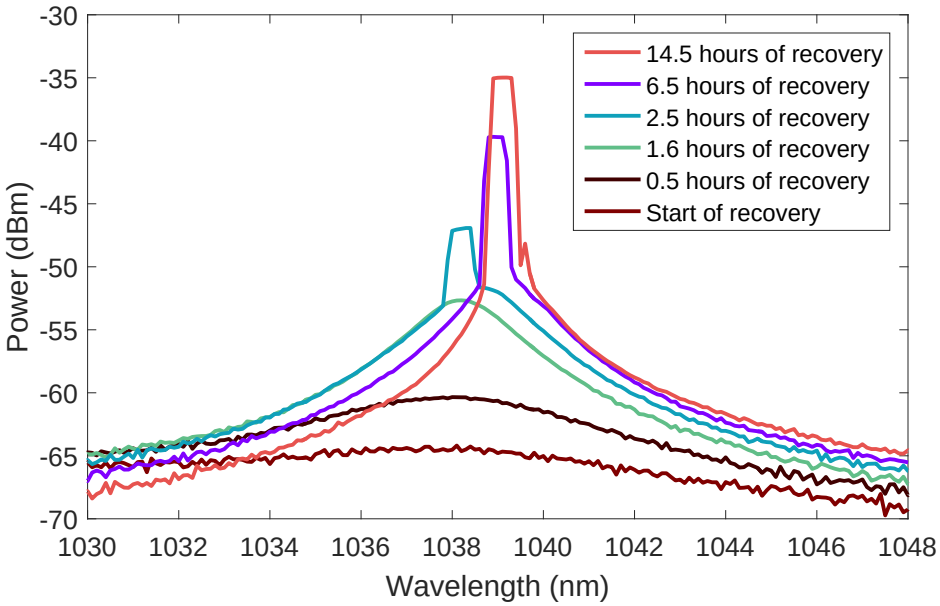


**Figure 20. The lasing wavelength of the YDFL at the start of recovery cannot be seen. As recovery time increased, the spectrum for the laser signal grew. At 2.5 hours of recovery time, a peak emerged at 1038 nm, then redshifted slightly at 6.5 hours of recovery time. After 6.5 hours, the peak of the YDFL signal did not shift any further.**

exposed to 145 krad(Si) of gamma radiation. Additionally, a third experiment was conducted on YDF2, exposing it to an additional 107 krad(Si) of gamma radiation after it was allowed to actively and passively recover for periods of time, 1.5 hours and 40 hours respectively. All three irradiation experiments exhibited exponential power decay of the YDFL as the total dose of gamma irradiation increased with time (32.3 krad/hr dose rate). Each of the three experiments suffered power losses of 13.7 - 17.3 dB/m. The third experiment showed the lasing wavelength of the YDFL completely extinguished as the total dose of gamma irradiation reached 252 krad(Si).

Active recovery data was taken immediately following each YDFs irradiation, as well as hours and days after irradiation. Each of the YDFs exhibited passive power recovery, at varied magnitudes. YDF1 saw passive power recovery each time the fiber was left dark for hours and days following irradiation. However, YDF2 saw only one instance of passive power recovery when it was left dark overnight.

However, YDF2 had one connector fiber re-spliced since it broke off during take-down upon completion of the third irradiation experiment. This is the most probable reason passive power recovery was not seen for the first time the fiber was left dark following its second irradiation dose. The active power recovery for both YDFs were similar. Each time the YDFs were placed back into the ring of the YDFL and the laser was turned on, the power would recover linearly with time. The rates at which the power recovered were much larger with the initial dose of 150 krad(Si), and the immediate recovery and next morning recovery rates for both YDFs were essentially the same. However, after allowing the fibers to sit dark for two days, the active recovery rates dropped by an order of magnitude, indicating a saturation of recovery had occurred.

# 5. Results of Gamma/Neutron Irradiation on an YDFL

## 5.1 Chapter Overview

Three experiments were conducted by operating an YDFL *in-situ* during exposure to mixed gamma/neutron radiation from the OSURR. The reactor was run at low power for reactor experiment 1, and full power for experiments #2 and #3. Each YDF, which connected to the YDFL by two 5 m passive patch fibers on each side, was placed in the thermal column (TC) of the reactor at two different positions and irradiated for 2.5 - 3.0 hours. The data collected from these experiments were continuous power output of the YDFL and spectral measurements from 650 to 1200 nm in half hour increments. Immediate recovery data was taken for reactor experiments #1 and #2. Recovery data could not be taken at any other time due to the fact that the connectors on the YDFs and the passive fibers absorbed large enough neutron doses that made them too radioactive to be released from the OSUNRL.

## 5.2 Experiment

### 5.2.1 Irradiation source description

The source for the reactor experiments was the OSURR, which is an open pool type reactor with several beam ports and dry tubes, a thermal column, and other irradiation facilities. For the reactor experiments conducted in this thesis, the reactor was operated at three different power levels. The first reactor experiment employed power levels of 50 W and 5 kW while the remaining two experiments were at full power (450 kW). The YDFs for each experiment were placed in the TC of the reactor to expose the fibers to thermal neutrons and gammas. At full reactor power, the TC had a maximum neutron flux of $10^{10}$ n/cm$^2$/s, but the irradiation rate for

the gammas was unknown. The neutron flux was reduced from the maximum value by placing the YDF further from the reactor's core within the TC. This was done for experiments #1 and #2, where the placement of the YDF is measured by how deep the YDF was placed from the outer wall of the TC. For experiment #1, the neutron flux was also reduced by operating the reactor at reduced power.

### 5.2.2 Experimental setup

The experimental layout for the irradiation experiments using the OSURR was the same as the layout used for the $^{60}$Co experiments. The type of YDF used was technically the same brand, Leikki YB1200-6/125DC; however, the YDF used for the $^{60}$Co experiments came directly from the manufacturer while the YDF used for the reactor experiments shipped from Thorlabs. This is mentioned because the current on the laser diode controller had to be increased from 650 mA to 1 A in order to achieve similar power output from the YDFL as seen with the $^{60}$Co experiments. Each YDF was placed in the graphite TC of the reactor with a 5 m length of passive fiber connected on each side of it. This allowed for the laser to be setup outside the TC, ensuring the YDF and the FC/APC connectors to the passive fibers were the only portions of the YDFL that received irradiation within the TC. Each YDF was placed at a predetermined position inside the TC. For each reactor experiment, the position and reactor power dictated the amount of neutron flux the YDF being irradiated would experience. For the first two reactor experiments, the YDF was placed 10.16 cm inside the TC, while the last reactor experiment was conducted at 50.8 cm inside the TC. The YDF was spooled into three 63.5 mm loops and taped to a flat piece of plastic that fit inside the TC that kept the YDF in place. The passive fibers were taped to the outside face of the TC to restrict the fibers from moving, and allowed for the metal door of the TC to slide in place

without pinching the fibers. Once the reactor was turned on it took about 25 minutes for it to achieve the desired power level for the experiment. For reactor experiment #1, the desired power was initially 50 W. After maintaining 50 W of power for an hour the reactor power was raised to 5 kW. For the final two reactor experiments, the reactor's operating power was set to the maximum power of 450 kW. The irradiation times for experiments #1, #2, and #3 were 2.5 hours, 2.5 hours, and 3.0 hours respectfully. All parameters for the reactor experiments have been summarized in Table 3 below. YDF4 was used twice because the last pristine fiber to be used for reactor experiment #3 was broken upon placing it in the TC. Since there was no way to fix the splice of the connector fiber to the pristine YDF, YDF4 was used instead.

**Table 3. Reactor experiments parameters**

| **Reactor Experiment #** | **YDF #** | **TC Position (cm)** | **Irradiation Time (hrs)** | **Reactor Power (kW)** | **Neutron Flux ($n/cm^2/s$)** | **Total n Dose ($n/cm^2$)** |
|---|---|---|---|---|---|---|
| 1 | 3 | 10.16 | 1 | 0.050 | $1\times10^5$ | $3.6\times10^8$ |
| | | | 1.5 | 5 | $1\times10^7$ | $5.4\times10^{10}$ |
| 2 | 4 | 10.16 | 2.5 | 450 | $1\times10^9$ | $9.1\times10^{12}$ |
| 3 | 4 | 50.80 | 3 | 450 | $1\times10^{10}$ | $1.1\times10^{14}$ |

### 5.3 Results and discussion

The output power of the YDFL was measured *in-situ* in order to determine the RIA through the YDF as it was exposed to a mix of gamma and neutron radiation. Also, spectral data was taken to observe how the radiation damage within the YDF affects the YDFL's spectrum, especially at the lasing wavelength. These results can then be compared with the results from the $^{60}$Co experiments to determine how radiation types, irradiation rates, and total doses affect an active YDFL.

### 5.3.1 YDF3 Irradiation - Reactor Experiment #1

The power degradation of the YDFL for the first reactor experiment was much lower than previously seen in the $^{60}$Co experiments. The YDFL's power before irradiation was 21.5 mW. During the 24 minutes it took to bring the reactor up to 50 W of power, the power from the YDFL decayed to 20.53 mW. The power for the reactor remained at 50 W for approximately one hour. During this time the power of the YDFL decayed only 0.7 mW, from 20.53 to 19.83 mW. The reactor was operated at 5 kW for the remaining two hours of the experiment. While the reactor power was increased by a factor of 100, the degradation of power seen in the YDFL remained slow, approximately 0.5 mW an hour. After two hours of irradiation time at the increased reactor power, the power of the YDFL reduced from 19.83 to 19.03 mW. The power of the YDFL versus the total neutron dose can be seen in Figure 21. The sharpest decrease in power for the YDFL in this experiment was seen as the reactor was brought up to power. The spectral data does not show a blueshift in the lasing wavelength of the YDFL as it did previously in the gamma only irradiation experiments. Figure 22 shows the spectrum of the YDFL at the lasing wavelength remains practically unaltered as the total neutron dose increased over time. Only the amplitude of the three main modes changed as the total dose increased.

### 5.3.2 YDF4 Irradiation - Reactor Experiments #2 and #3

#### 5.3.2.1 First Irradiation - Reactor Experiment #2

The initial power of the YDFL with a pristine YDF (YDF4) positioned 10.16 cm deep in the TC was 23.48 mW. The reactor took 22 minutes to achieve maximum power, during which the YDFL decreased in power by 0.68 mW. After the maximum reactor power was achieved, the YDFL began to decrease at a higher rate compared to the first reactor experiment. The neutron flux for reactor experiment

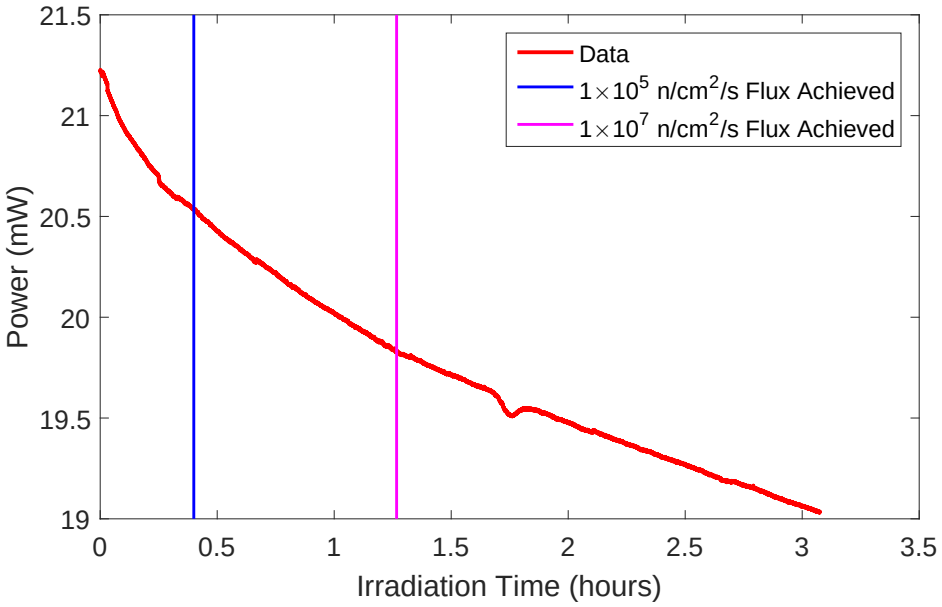


**Figure 21. A continuous decrease in power was seen for both reactor power levels of 50 W and 5 kW. The blue vertical lines represent the time at which the desired power levels were achieved. The sharpest decrease in power happened after the reactor was turned on and brought up to power. After the reactor attained 50 W of power, the degradation in the YDFL power slowed from the initial degradation slope. Once the power in the reactor reached 5 kW, the power degradation in the YDFL remained roughly the same as it was for the reactor power of 50 W. The dips in YDFL power at the 0.25 and 1.75 hour marks are uncharacteristic of previous gamma only irradiation data. However, the power recovers and follows the slopes previously seen.**

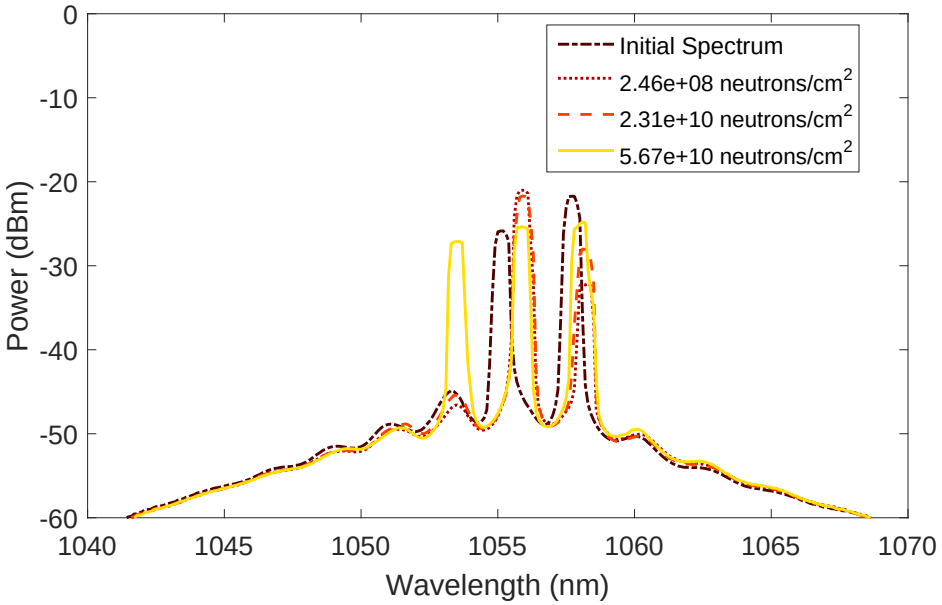


**Figure 22. The peaks of the individual modes in the YDFL changed in amplitude, but the wavelength did not shift significantly as the total dose increased in YDF3 for reactor experiment #1.**

#2 was roughly 2 and 4 orders of magnitude greater than the fluxes used in the first reactor experiment. The YDFL was irradiated for approximately 2.5 hours with a neutron flux of 1 $\times 10^9$ n/cm$^2$/s which caused RIA in the YDF of 0.65 dB/m. The RIA for all three reactor experiments is shown in Figure 23. The spectral data for experiment #2, shown in Figure 24, exhibited the least amount of change for all three reactor experiments. Only small amplitude changes were seen in the lasing modes for the YDFL, with the most significant change being 15 dB/m in the peak amplitude of the furthest mode to the right.

#### 5.3.2.2 Second Irradiation - Reactor Test #3

The final reactor experiment utilized the highest possible neutron flux within the TC, which was the highest neutron flux used for the three reactor experiments, of 1 $\times 10^{10}$ n/cm$^2$/s. This final experiment for the reactor experiments mirrors the third experiment performed in the $^{60}$Co irradiation chamber as it takes the YDF irradiated from the previous experiment and re-irradiates it. This happened out of necessity as the last available pristine YDF was broken apart (FC/APC connector fiber splicing broke) attempting to position it within the TC. Therefore a previously irradiated YDF (YDF4) had to be substituted for this experiment. This YDF had already received a neutron dose of 9.1 $\times 10^{12}$ n/cm$^2$ from the previous experiment. For its re-irradiation, YDF4 was placed deeper within the TC at 50.80 cm to achieve the highest neutron flux possible. The YDF was then irradiated for three hours and the degradation in power was continuously monitored with spectral data taken in half hour increments. During this experiment the RIA within the fiber increased from 0.9 to 6.3 dB/m. Despite the fact that this experiment was a re-irradiation of YDF4, the RIA increased at a similar rate to reactor experiment #2 (once the total neutron dose in the YDF had exceeded $10^{12}$ n/cm$^2$). This

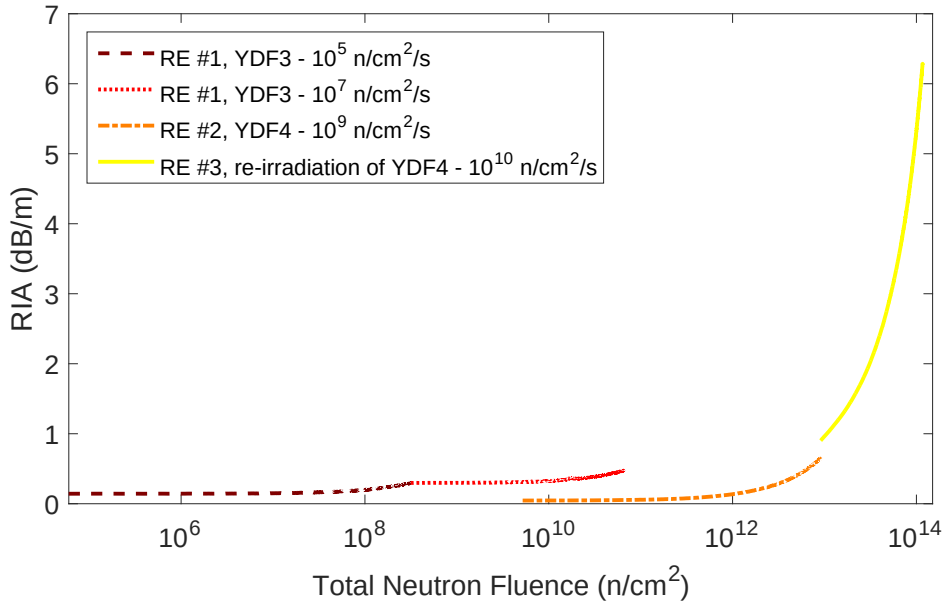


**Figure 23. Radiation induced attenuation for all three reactor experiments (RE #1 - RE #3). YDF3 was exposed to the smallest neutron flux of 1 $\times 10^5$ and 1 $\times 10^7$ n/cm$^2$/s. While the final two experiments had increased fluxes of 1 $\times 10^9$ and 1 $\times 10^{10}$ n/cm$^2$/s respectfully. The RIA increases slowly as the total neutron dose increases from $10^5$ up to $10^{12}$ n/cm$^2$/s. At this point the RIA begins to increase rapidly up to the total neutron dose of 1.2 $\times 10^{14}$ n/cm$^2$.**

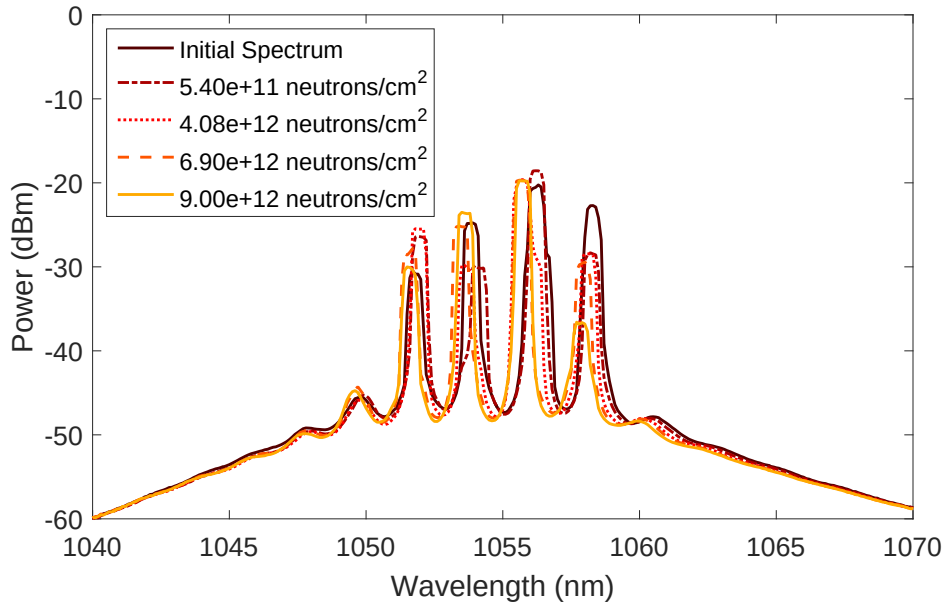


**Figure 24. The peaks of the individual modes in the YDFL slightly changed in amplitude, but no wavelength shifting occurred as the total dose increased in YDF3 for reactor experiment #2.**

comparison can be seen in Figure 23. The spectral data for reactor experiment #3 was the least similar to the spectral data from the previous two experiments. The modes of the laser were not as well defined for the YDFL here as they were previously for the first two reactor experiments (see Figure 25).

### 5.3.3 Temperature dependence of absorption

The temperature of the fibers in an YDFL have a significant effect on how the laser performs and is characterized. According to Moore's study in 2011, the absorption coefficient increases with increasing temperature for wavelengths in the 1000 - 1120 nm range and decreases for wavelengths in the 900 - 1000 nm range [37]. For a temperature increase from 26 °C to 80 °C the absorption for 1060 nm increased 1.5 dB/m. When the temperature of the fiber was >600 °C there was a much larger absorption of 15 dB/m. The reduction in population inversion of the ${}^2F_{5/2}$ level is responsible for the increased absorption by reducing the number of transitions at the 1010 - 1100 nm range (see Figure 2). The reduction in population inversion occurs from the temperature increase of the fiber. The thermal energy added by heating the fiber causes the ions in the ground state to thermally excite to the middle levels in the ${}^2F_{7/2}$ level, thereby reducing the amount of ions available in the ground state that can be pumped by the pump laser into the upper excited ${}^2F_{5/2}$ level.

The temperature of the TC for the OSURR was not actively controlled nor monitored during the reactor experiments. Due to its distance from the reactor and the inherent openness of the TC itself, it was assumed that the temperature of the YDF in the TC was the same ambient temperature of the facility, roughly 19 °C. Since there was little to no change in temperature of the facility during the reactor experiments, it can be assumed that there was no temperature induced increase of

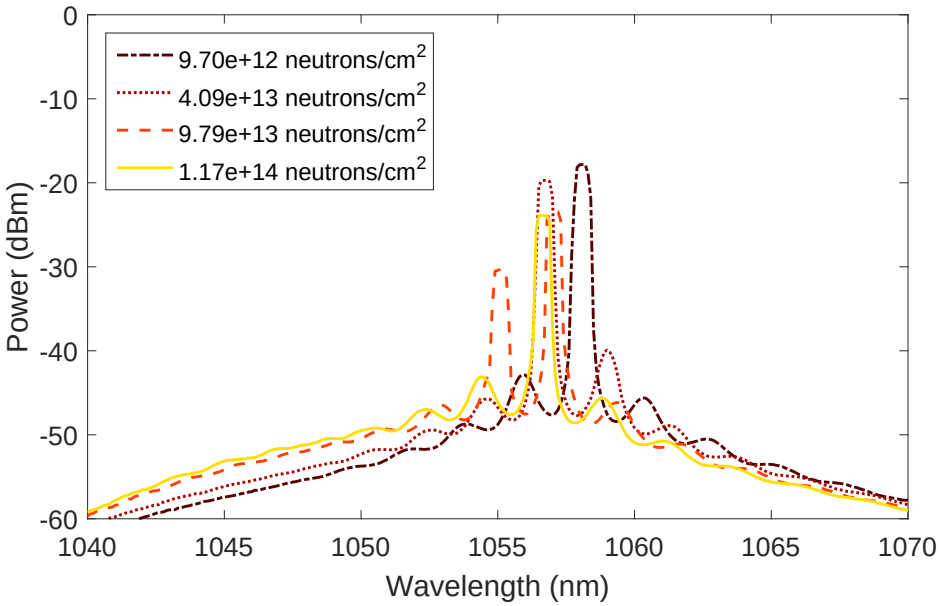


**Figure 25. The peaks of the individual modes in the YDFL slightly changed amplitude, but no wavelength shifting occurred as total dose increased in YDF3 for reactor experiment #3.**

absorption at the signal wavelength for the YDFL.

## 5.4 Recovery Data

Recovery data for the first two reactor experiments were taken. The time frame for the recovery data was quite limited due to the scheduling of reactor time and the inability to remove the YDFs from the OSURR due to their radioactivity. Therefore, the reactor recovery data will not be easily comparable to the $^{60}$Co recovery data since the recovery data collection times were significantly shorter and less conclusive. However, the setup for the recovery data is similar to the process in which the $^{60}$Co recovery data was collected. The YDFL remained on during the five minutes it took the reactor to shut down. Once the reactor completed shut down, the recovery data was recorded with everything still in place as it was for the irradiation (no movement of fibers like there was in the $^{60}$Co recovery data).

### 5.4.1 YDF3 - Recovery Data

Recovery data for the first reactor experiment was only conducted immediately following the irradiation of YDF3. Data was collected for 56 minutes, seen in Figure 26; during this time, the power in the YDFL continued to decline as it had when it was being irradiated with mixed neutron and gamma radiation. The decay in power seen below was roughly 0.3 mW/hr, which was close to the 0.5 mW/hr power decay rate seen while the YDF was being irradiated. At the 20 minute mark there was a spike in power of the YDFL, from 18.90 to 19.01 mW, but then the power continued to decay at the same rate. Twenty minutes later, there was a sharp decrease in power which seemed to be a resetting of the previous spike in power. The power decay rate remained constant throughout the recovery data despite the spike and subsequent drop in power. No other recovery data could be collected for YDF3.

### 5.4.2 YDF4 - Recovery Data

Recovery data was taken for reactor experiment #2 immediately after YDF4 was irradiated and during the following morning (18.5 hours post-irradiation). For the 28 minutes of active recovery done immediately following irradiation, the power of the YDFL increased 50 $\mu$W after about five minutes. After the initial, slight power gain, the power stayed at the same level of 20.2 mW for the remainder of that recovery session until the YDFL was shut off. The following morning, when the YDFL was turned back on, the initial power reading was 21.1 mW, up 0.9 mW from the previous day. However, the power quickly dropped 0.5 mW within the first two minutes of active recovery. Following this point, the power continued to decay more slowly to 20.45 mW over the course of 25 minutes. Just prior to the conclusion of this recovery session, the power spiked up 0.20 mW and then leveled off at 20.6 mW for the last two minutes of the session. This seems to be an anomaly as it was not

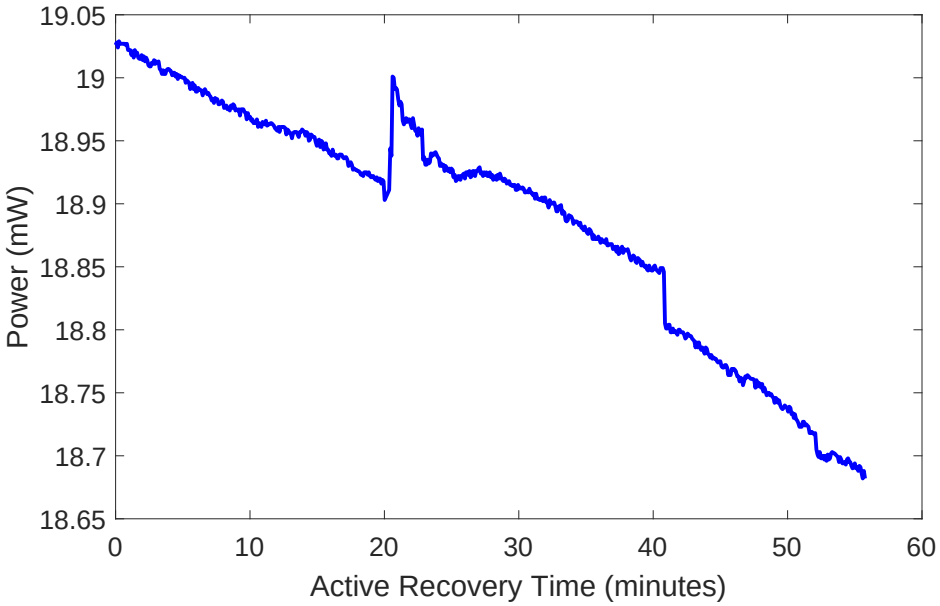


**Figure 26. The immediate recovery data following reactor experiment #1 shows a continuing decrease in power over the course of 55 min, despite a spike and subsequent drop in power 20 min later. The YDFL does not experience a recovery in power because the connectors on the YDF absorbed enough radiation to be radioactive themselves. The decay in power seen here is roughly 0.3 mW/hr, which is close to the 0.5 mW/hr power decay rate seen during irradiation.**

seen in any other of the experiments.

### 5.5 Summary

The degradation in power of the YDFL was measured continuously for three separate experiments where two YDFs were exposed to irradiation from a mixed gamma and neutron source at the OSURR. The OSURR is a mixed gamma/neutron irradiation source, however, only the neutron flux was known for the TC. The neutron flux was controlled by placement of the YDF in the TC and the power of the reactor. Each reactor experiment was run between 2.5 - 3.0 hours. The flux for each of the three reactor experiments were as follows: $10^5$ and $10^7$, $10^9$, and $10^{10}$ n/cm$^2$/s. Other parameters for each reactor experiment has been summarized in Table 3. Each of the irradiated YDFs showed a steady increase in

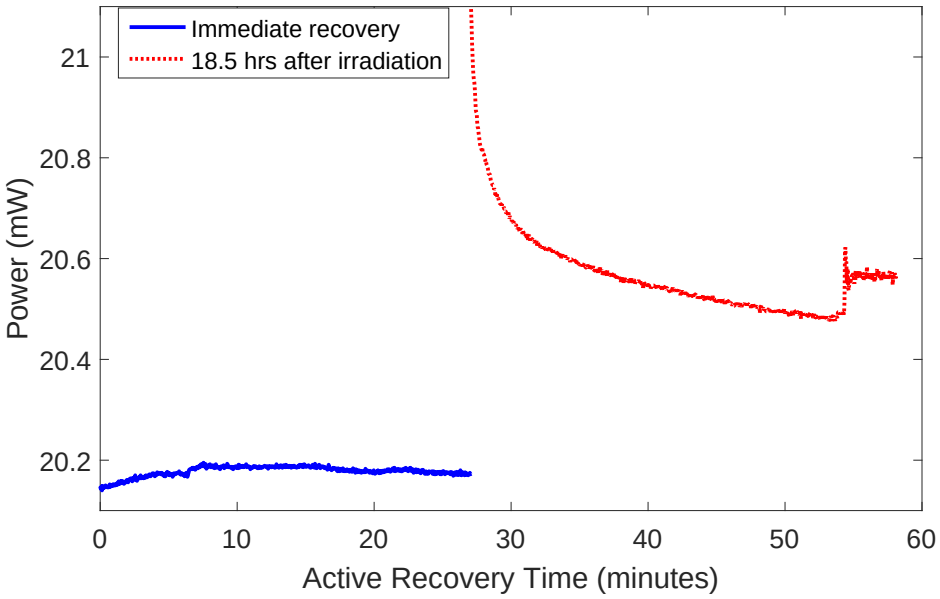


**Figure 27. The immediate recovery data for reactor experiment #2, where YDF4 was exposed to a total neutron dose $9.1\times10^{12}$ n/cm$^2$, shows an increase in power of 50 $\mu$W over the first 6 minutes. For the remaining 20 minutes, the power levels out and no longer recovers. The recovery data for the following morning shows a passive recovery of 1 mW once the laser was turned back on. However, the power drops sharply within the first minute and then continues to decay until the 55 minute mark. At the 55 minute mark the power spiked up 0.2 mW and then leveled out for the last 2 minutes of data.**

RIA with an increase in total neutron dose over time. The increase in RIA with the reactor experiments were consistent with one another, but the RIA was roughly half of what was experienced in the $^{60}$Co experiments.

For the first two reactor experiments, immediately following the shut down of the reactor, the YDFL remained on and recovery data was collected. YDF3 was allowed to actively recover for 56 minutes, while YDF4 was allowed to actively recover for a total of 58 minutes between two days. The recovery data for these reactor experiments did not show significant annealing as seen in the $^{60}$Co recovery data. The power for both YDFs continued to decrease during the active recovery times. However for YDF4, a slight power increase of 50 $\mu$W was observed within the first 6 minutes of active recovery. This was likely due to an increase in temperature of the fiber as the light was passing through it. The continued power degradation seen is likely due to the connectors on the YDF and passive fibers had absorbed enough radiation to become radioactive themselves. Measurements were taken with a Geiger counter to determine the radioactivity of the connectors, either immediately following the experiment (experiment #1) or the next morning (experiment #2), and for both experiments they measured approximately 6 - 10 mrem/hr.

# 6. Analysis and Conclusions

## 6.1 Comparing Results with Experiments from Literature

The focus of this thesis was to supplement existing literature on RE-doped fibers that did not include radiation sensitivity experiments on active YDFLs. The power degradation on an active YDFL caused from irradiation by gamma and mixed neutron/gamma radiation was recorded. The power loss seen was consistent with several other published results on RE-doped fibers and fiber optic systems in both passive and active configurations. Exact comparisons cannot be made with the experimental results from this thesis to other published results due to many factors that differed between experiments. Some, but not all, examples of how the experiments differed from the experiments presented in this thesis include the following: the type of RE-dopant used in the silica, doping concentrations, fiber core and cladding sizes, doped fiber length, irradiation rate, total dose, passive or active configurations, etc. Therefore, only rough comparisons were made concerning the trend of power decay, the RIA seen within the RE-doped fiber/amplifier/laser, and active and passive recovery rates.

In each irradiation experiment conducted for this thesis, increasing the total dose resulted in the loss of power. The power decayed exponentially as the total dose increased linearly over time. This exponential decrease in power is in agreement with other published results on the irradiation of RE-doped fibers and/or amplifiers. For example, Fox et al. published results in 2009 of an active YDFA irradiated with a $^{60}$Co gamma source at a rate of 0.116 rad(Si)/s. Fox reported an exponential decrease in power of the signal wavelength from 780 mW to 137 mW after a total dose of 7.6 krad(Si) was achieved [17]. This equates to a RIA of 2.52 dB/m. The RIA seen in Fox's experiment was much higher than the RIA for the YDFL seen in

the experiments conducted for this thesis by roughly 1.7 dB/m. The difference could be from the type of YDF used, the length of the fiber used (3 m for Fox compared to 1 m for this thesis), or the difference in dose rate (Fox's rate was quite low). Table 4 summarizes the results of gamma irradiation experiments conducted in this work (t.w.) as well as results from other published experiments on RE-doped fibers and systems. It was thought that irradiating the YDFL while it was actively lasing would help to prevent the creation of certain color centers within the fiber, thereby reducing the RIA over time. However, the degree to which this occurred was hard to determine since there was a lack of similarity between other published experiments.

Table 4 also compares the RIA from this thesis at each total dose (TD) achieved in each experiment in the table (last column). The last column, with the exception of the second row, shows the values for YDF1 and YDF2 separated by a slash (/). The RIA for YDF2 after a total dose of 200 krad(Si) was calculated to compare with the results from Fox, et al. in 2007 [38]. This was done by adding the RIA from the first irradiation of YDF2, at a total dose of 145 krad(Si), to the RIA of YDF2 seen at 200 krad(Si). The data from which these results were derived can be seen plotted in Figure 18. Analysis for this figure used the initial power reading of the YDFL, just before the experiments began, as the $P_{in}$ values for calculating RIA using equation 3. The power of the YDFL at the beginning of each experiment was used, rather than the initial power of the YDFL from experiment #2. If each initial power measurement had been used, a discontinuity between the RIA at the end of experiment #2 and the beginning of experiment #3 would have been seen (since the power had recovered some, decreasing RIA). YDF2 was the only fiber to receive a total dose greater than 145 krad(Si); this information is recorded in the last column in the second row in Table 4.

The RIA for the YDFL was higher than some results and lower than other

**Table 4. Gamma irradiation experimental results compared**

| Reference Year Citation | RE-dopant and Configuration | Dose Rate rad(Si)/s | Total Dose krad(Si) | RIA at TD dB/m | T.w.'s RIA at current row's TD |
|---|---|---|---|---|---|
| Fox 2009 [17] | Active YDFA | 0.116 | 7.6 | 2.5 | 0.744/0.851 |
| Fox 2010 [39] | Passive YDF | 40.1 | 35 | 4.2 | 3.6/3.7 |
| Girard 2012 [11] | Active EDFA | 0.3 | 35 | 0.5 | 3.6/3.7 |
| Alam 2007 [18] | Active EDF | 4.5 | 91.0 | 23 | 8.3/9.3 |
| Singleton 2014 [2] | Active YDFA | 6/11 | 100 | 1.4-4.0 | 9.3/10.5 |
| Poulin 2016 [t.w.] | Active YDFL | 9 | 145 | 14-17 | **YDF1/YDF2** |
| Fox 2007 [38] | Passive E/YDF | 14.3/40.1 | 200 | 16 | -/21.3 |

results published in the literature, which are shown in Table 4. For example, the RIA in the data from this work was much higher than the RIA published by Singleton, but lower than the RIA published by Fox. Singleton's experiments in [2] determined the radiation sensitivity of YDFs similar to those used in the experiments from this thesis. However, the fibers were configured as an active YDFA as opposed to an active YDFL, and the YDF she used had a core size of 20 $\mu$m rather than the 6 $\mu$m core used in this work. In this case, the YDFs exhibited less radiation sensitivity when configured as an amplifier than when configured as a laser. Conversely, the results published by Fox in [39] on passively irradiated YDFs showed higher radiation sensitivity than that of the active YDFL irradiation data presented in this thesis. However, because experimental configurations and doped-fiber characteristics differed between the experiments used for comparison, no trends or correlations between the results in Table 4 are evident, other than the exponential decrease in power due to an increase in total dose previously mentioned.

There were relatively few publications in the literature on mixed gamma/neutron irradiation experiments to which the results from this thesis could be compared. Lezius et al. published results in 2012 of neutron irradiation on active EDFs with a

neutron flux of roughly $3\times10^4$ n/cm$^2$/s. His results showed a shallow exponential increase of RIA, less than 1%, with a total neutron dose of about $5\times10^8$ n/cm$^2$ [6]. The neutron flux varied from $1\times10^5$ - $1\times10^7$ n/cm$^2$/s for the first experiment conducted on the YDFL with the OSURR. However, the neutron radiation produced by the reactor also contained an unknown amount of gamma irradiation. The RIA for this experiment on the YDFL was 0.47 dB/m after a total dose of $5.4\times10^{10}$ n/cm$^2$. These results align to some degree with the results and conclusions drawn from Lezius et al., specifically, that the neutron irradiation degrades the transmission through the fiber very weakly. The higher values for the results published here may be due to the neutron irradiation being mixed with an unknown amount of gamma irradiation from the reactor causing a higher RIA in the YDFL. However, the neutron flux of Lezius' experiment was also an order of magnitude smaller than the first reactor experiment presented here. It's also important to note that the energy of the neutrons in Lezius' experiment were 20 and 180 MeV while the neutrons for the reactor experiments presented in this thesis were less than 0.5 eV. The higher energy neutrons used in Lezius' experiment would react less with the fiber during irradiation, therefore producing less absorption in the fiber.

## 6.2 RIA Power Law Fit

### 6.2.1 Gamma Only Experiments

The power law fit is a common method to model the RIA seen from irradiation of the fiber [2, 6, 8, 40, 41, 42, 43] . The power law, shown in equation 5, is a function of the radiation dose, $D$, and is dependent on two variables, $\alpha$ and $\beta$ , that are specific to the type of fiber used.

$$RIA(D) = \alpha D^{\beta} \tag{5}$$

The RIA within the YDFL was calculated from the power measurements and the results from the gamma only experiments will be discussed and analyzed. The RIA for experiments #1 and #2 were 17.16 and 13.62 dB/m with a total dose of 145 krad(Si), and the RIA for experiment #3 (the re-irradiation of YDF2) was 17.35 dB/m with a total dose of 250 krad(Si). The power law fit for gamma only experiments #1 and #2 are shown in Figure 28. The value for $\beta$ was varied from 0.7 - 1.0 in order to find the smallest difference of $\alpha$ values for each of the first two gamma only experiments. This was accomplished when $\beta$ was set to 1.0 and the delta of the $\alpha$ values was 0.0152. The $R^2$ values for the power law fitted to the RIA data were 0.9935 for experiment #1, and 0.9978 for experiment #2.

The power law fit for Experiment #3 will be analyzed two different ways. The first case, case #1, will be fit to the power law using the true total dose that YDF2 was exposed to. This means the dose from the previous experiment (145 krad(Si) from the first irradiation of YDF2) was included. Case #2 was constructed to compare, using similar conditions, the power law fit from experiment #3 with the power law fits from the previous two experiments. This was done by adjusting the conditions for how the data was presented. This was done by excluding the total dose from the previous experiment (experiment #2). In other words, the gamma dose for the start of experiment #3 was set to 0 krad(Si), and the RIA was calculated so the initial power measurement of the YDFL just before re-irradiation was used as the $P_{in}$ value in equation 3. Doing this set the RIA to 0 dB/m at the beginning of the experiment #3 for this case.

The power law fit for case #1 of reactor experiment #3 did not fit as well to the RIA data as the first two reactor experiments did. For case #1, the value of $\beta$ was limited to the range of 0.7 - 1.0, but fit best at 0.9591, while $\alpha$ was fixed to 0.1209, the same value of $\alpha$ used in the power law fit from experiment #2. The goodness of

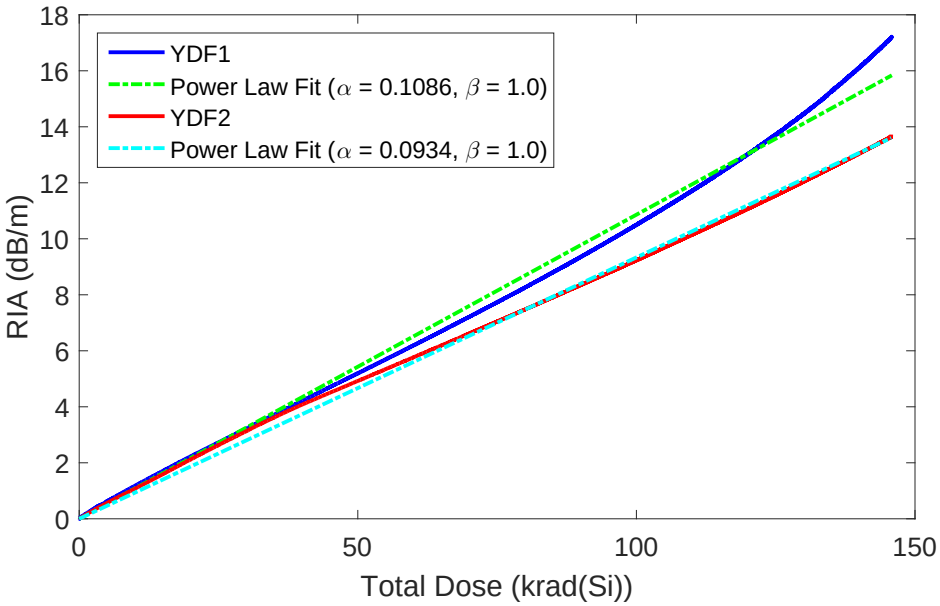


**Figure 28. The power law fits for YDF1 and YDF2 with $\beta$ fixed at 1.0. The difference between the $\alpha$ values for each YDF was the smallest when $\beta$ was set to 1.0. Therefore, there is high confidence that the power law is a good model for the YDF used in these experiments up to a maximum dose of 150 krad(Si).**

fit, the $R^2$ value, was 0.7859, and is shown in Figure 29.

The goodness of fit for the power law fit to RIA in case #2 was higher than case #1. The $R^2$ value improved to 0.9816. This value was achieved by setting $\beta$ to 1.0 and fixing $\alpha$ to 0.1209, the value which was used in the power law fit for experiment #2. The power law fit versus RIA for case #2 can be seen in Figure 30.

Upon completion of experiment #2, YDF2 was allowed to actively and passively recover for 2 and 30 hours respectively. This recovery period reduced the RIA by 2.65 dB/m and likely repaired some of the unstable color centers (shorter lifetimes). The unstable color centers require less energy to be annealed than other color centers that have longer lifetimes. Both passive and active recovery occurred in the gamma only recovery experiments. In these recovery experiments, passive recovery occurred at room temperature over the course of 18 and 90 hours, resulting in power recovery of 100 and 550 $\mu$W respectively. Furthermore, the active recovery resulted in much higher gain over the course of several hours. This was seen in active

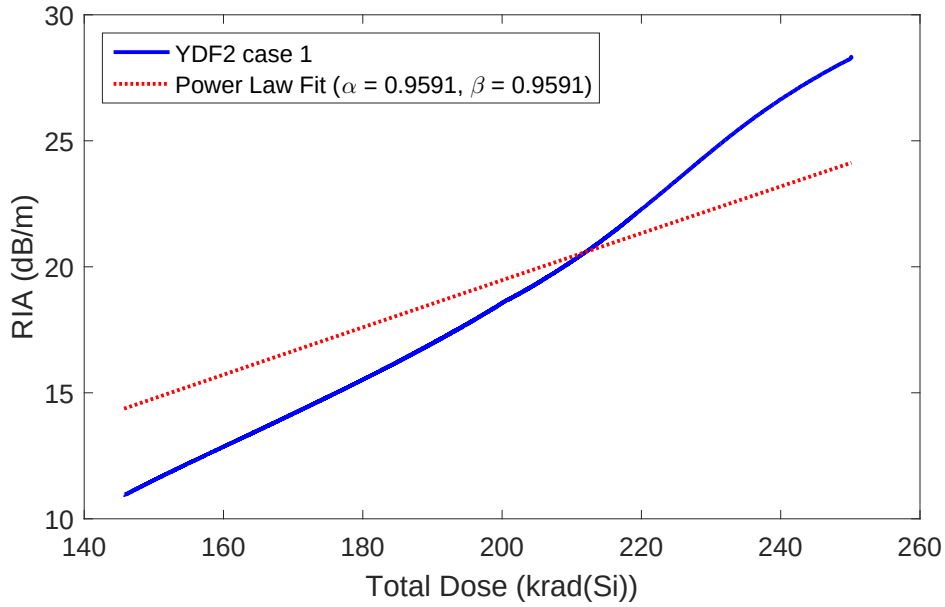


**Figure 29. Experiment #3, the re-irradiation of YDF2, with the total dose from the previous experiment, the first irradiation of YDF2, included (case #1). The value of $\beta$ was limited to the range of 0.7 - 1.0, but fit best at 0.951, while $\alpha$ was fixed at the experiment #2 value of 0.1209. These conditions produced an $R^2$ value of 0.7859, which was the worst fit for all of the gamma only experimental analysis.**

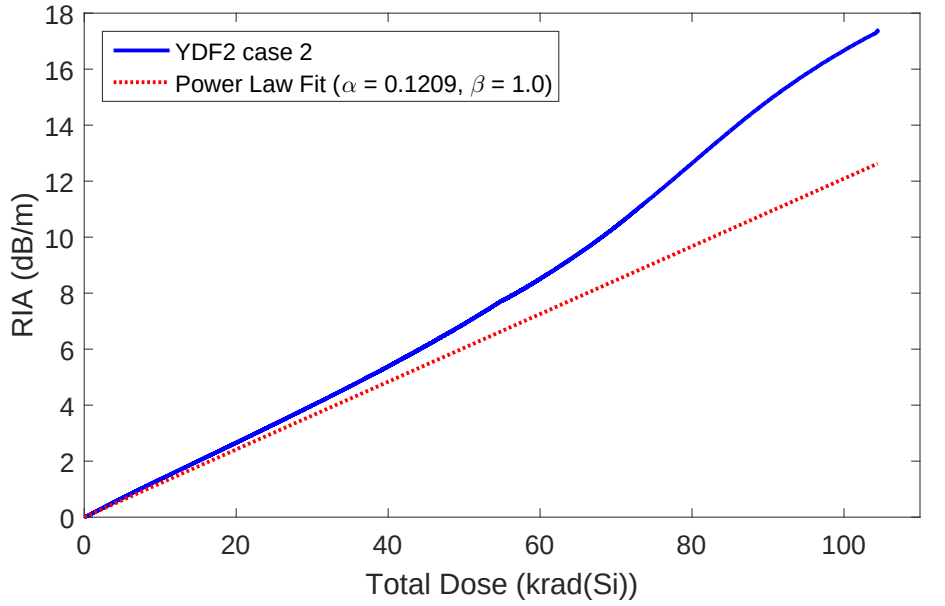


**Figure 30. Experiment #3, the re-irradiation of YDF2, with the total dose from the previous experiment, the first irradiation of YDF2, excluded (case #2). Using these parameters, the power law fit improved with an $R^2$ value of 0.9816 compared to the fit produced when the gamma dose from experiment #2 was included. For this case, the best fit occurred with $\beta$ set to 1.0, with $\alpha$ again fixed to 0.1209, the value which was used in the power law fit for experiment #2**

recovery experiment #1, when the YDFL was turned back on after being off for 18 hours (where it passively recovered 100 $\mu$W of power). Within the first 10 minutes of the YDFL being back on the power increased 100 $\mu$W. This was the same power recovery seen over a passive recovery period, but in 9.3% of the time. This implies that adding energy to the YDF, in this case allowing it to lase, decreases the time it takes for the unstable color centers to return to the ground state on their own. The fact that the color centers get repaired at higher rates when the YDFL is on might be the reason the RIA was less than what the power law predicted, up to a total dose of 210 krad(Si), for case #1. Following this total dose, the RIA becomes higher than the predicted values with the power law. This suggests that the fiber dependent variables, $\alpha$ and $\beta$, of the power law may need to be adjusted as the total dose exceeds 210 krad(Si).

Another point can be made when comparing the power law fits for experiment #1 and #2 to the respective RIA data. The power of the YDFL was 7.4 mW higher for experiment #2 than it was for experiment #1. The increased power of the YDFL in experiment #2 could be the reason why the RIA in experiment #2 was lower than the RIA in experiment #1. Both of these experiments were conducted exactly the same, including the current and temperature settings of the pump laser's controller. The only difference was the initial power of the YDFL with its respective YDF connected as the gain medium. The increased power must help to prevent the creation of certain (less stable) color centers within the YDF through bleaching, and could also have repaired more color centers (from actively lasing) with short lifetimes during the irradiation.

### 6.2.2 Mixed Gamma/Neutron Experiments

The power law was used to model the RIA for the given neutron fluence for each mixed gamma/neutron experiment (reactor experiments), and the power law accurately modeled the RIA for reactor experiments #2 and #3. The power law did not fit well to the RIA calculated for reactor experiment #1 when $\beta$ was restricted to the 0.7 - 1.0 range. In order for the power law to best model the RIA seen in reactor experiment #1, the restriction on $\beta$ had to be removed. The values for $\beta$ that provided the best fit for the power law to the RIA data was 0.2366 and 0.1498 for neutron fluxes of $10^5$ and $10^7$ n/cm$^2$/s respectively. The values of $\alpha$ for these two power law fits were 0.0027 and 0.0107. The $R^2$ value for these two power law fits were 0.9068 and 0.8885, and is shown in Figure 31. The neutron flux was very low in this experiment, and while the gamma dose rate was unknown, the data proves that it too was quite low. This is why the power law does not fit well using the typical constraints on $\beta$. There was not enough gamma radiation present to produce a high enough concentration of color centers to cause $\beta$ to fall between 0.7 - 1.0. The power law, under this constraint, must have some minimum gamma dose rate in order to accurately predict the RIA that will occur from irradiation.

The power law fit to the RIA seen in reactor experiments #2 and #3 are shown in Figures 32 and 33 respectively. The value for $\beta$ was varied from 0.7 - 1.0 in order to find the smallest difference in $\alpha$ between these two experiments. The value of $\beta$ where this occurred was 0.975. This resulted in a difference in the $\alpha$ values of $4.0\times10^{-14}$. The $R^2$ value for the Power Law fit to the RIA were 0.9553 and 0.9844 for experiments #2 and #3 respectively. Because the $R^2$ value is high for both experiments, the Power Law fit using the specified values of $\alpha$ and $\beta$ for the YDF used in this thesis is a good model to predict RIA at the neutron fluences utilized in these two experiments.

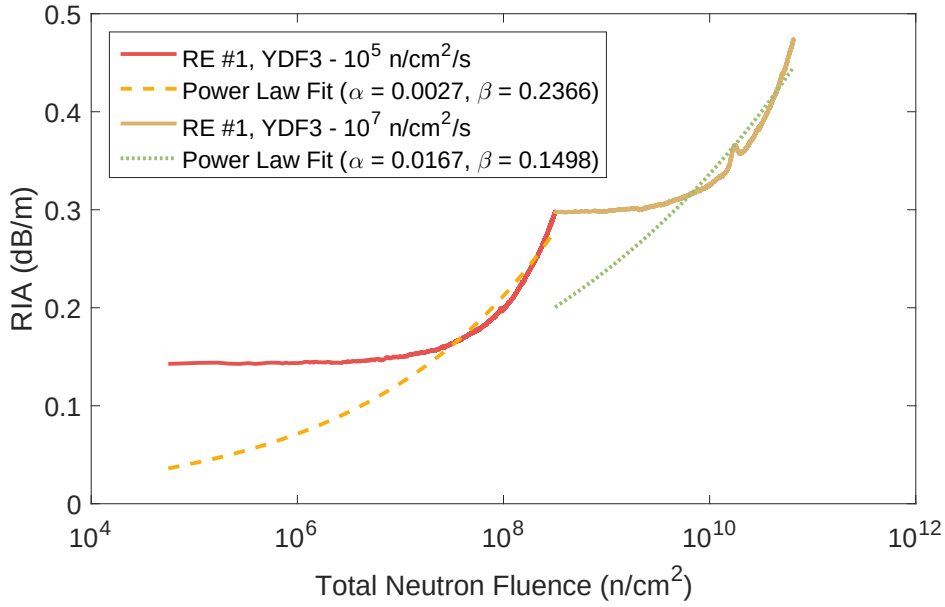


**Figure 31. The power law fits for reactor experiment #1. In order to get an $R^2$ value above 0.50, the values for $\beta$ could not be restricted in the normal range of 0.7 - 1.0, as was done in all other instances. The reduced value of $\beta$ for the power law fits here show that the low neutron fluxes for this experiment do not cause a significant number of color centers to be produced within the YDF.**

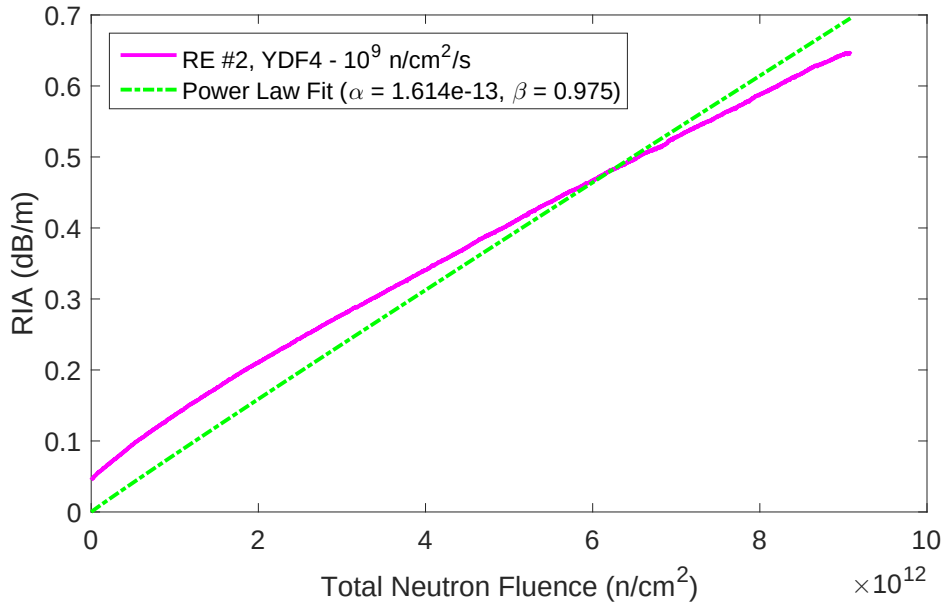


**Figure 32. The power law fit has a goodness of fit to the actual RIA data of 0.9553. The value for $\beta$ was allowed to vary from 0.7 - 1.0 and the final value used was determined by which $\beta$ gave the closest two values of $\alpha$ between experiments #2 and #3. The value for $\beta$ where this occurred is 0.975.**

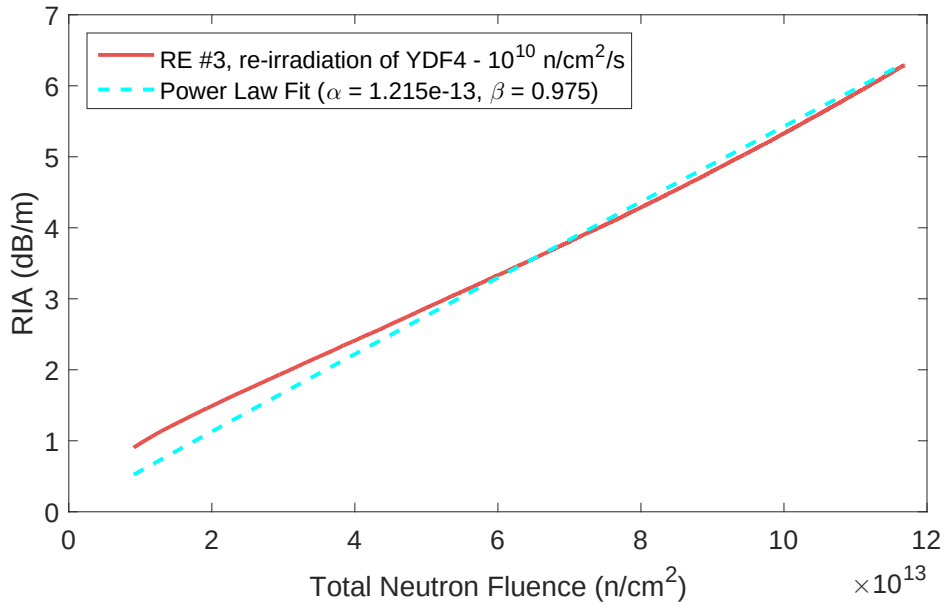


**Figure 33. The power law fit has a goodness of fit to the actual RIA data of 0.9844. The value for $\beta$ was allowed to vary from 0.7 - 1.0 and the final value used was determined by which $\beta$ gave the closest two values of $\alpha$ between experiments #2 and #3. The value for $\beta$ where this occurred is 0.975.**

## 6.3 Spectral Analysis

Analysis of the spectra data collected by the OSA in the gamma only experiments helped determine the affect of radiation on the YDFL. The pre-irradiation spectrum of the lasing wavelength of the YDFL was approximately 20 nm in width, indicating there were several modes lasing simultaneously. After a total dose of 145 krad(Si), the lasing wavelength of the YDFL blueshifted a total of 13 and 15 nm for YDF1 and YDF2 respectively. Additionally, the pre-irradiated spectrum and the irradiated spectrum with a total dose of less than 75 krad(Si) indicated significant ASE, especially in the 1045 - 1055 nm range. The peak of the lasing wavelength sharpened after a total gamma dose of 75 krad(Si). The cause of this sharpening is likely from the formation of color centers that are specifically absorbing the pump signal, thereby reducing the amount of excited $Yb^{3+}$ ions within the YDF. With less excited $Yb^{3+}$ ions in the YDF, the amount of ASE

within the YDFL is reduced. Finally, the spectra data of the YDFL evidenced the termination of the lasing peak after the YDF was exposed to a total dose of 230 krad(Si). This may be due to the production of color centers in the fiber, which absorbed enough of the pump signal and lasing signal to prevent the cascading effect (photon multiplication from stimulated emission) from occurring.

The spectra data for the reactor experiments, unlike the gamma only experiments, did not exhibit any significant shifting in wavelength of the YDFL. Instead, there were 3-5 significant lasing peaks in the spectrum that exhibited slight increases or decreases in power, but no shifting. Only in the third reactor experiment did a slight 0.5 - 1.0 nm blueshift occur in the lasing wavelength. Although the dose rate for the gamma radiation in the reactor experiments was unknown, analysis of the spectra data for these experiments indicated the gamma dose rate must have been significantly less than the 32.7 krad(Si)/hr dose rate produced in the gamma only experiments. The neutron radiation is not a significant source for creation of color centers in the YDFL. This is evidenced by the low RIA produced in all three reactor experiments. The highest RIA from the mixed gamma/neutron experiments, specifically from reactor experiment #3, was roughly 1/3 - 1/2 of the RIA reported from the gamma only experiments.

### 6.4 Active Recovery Analysis

The purpose of the active recovery experiments was to determine the rate at which color centers in the YDFL were repaired (annealed) at room temperature. When the color centers are repaired, the trapped electrons in the silica lattice are removed, which in-turn, reduces the amount of RIA in the fiber. Only the active recovery data collected from the YDFs irradiated by the $^{60}$Co gamma source will be analyzed below. The recovery experiments that immediately followed irradiation

from the OSURR did not experience any significant power recovery. Furthermore, the YDFs irradiated by the OSURR could not be moved to the lab for several weeks due to OSU's radioactive safety constraints. This prevented any further active recovery experiments for the YDFs irradiated by the OSURR in this thesis.

The active recovery data for YDF1 and YDF2 was analyzed at various points following the irradiation experiments. The goal was to determine how long it would take the YDFL to actively recover all of the power lost from radiation damage. While the YDFL was never left on long enough to achieve full power recovery, the time it would take to recover fully was estimated by determining the slopes (recovery rates) from the recovery data in Figures 11 and 14. These recovery rates and the calculated recovery times are summarized in Table 5. The recovery rates for each YDF diminished as the number of days after irradiation increased. The exception to this was the active recovery experiment performed the morning after the irradiation of YDF1 (labeled "Next morning recovery" in Table 5). This experiment experienced a higher recovery rate when compared to the rate immediately following irradiation. The active recovery time for the "Next morning recovery" experiment was only 20 minutes, the shortest active recovery time for all recovery experiments. Also, the recovery rate for the last recovery experiment on YDF2 was basically the same recovery rate seen on the previous day. This shows that there is a saturation of the active recovery rate at room temperature. The saturation of recovery likely stems from the lifetimes of the color centers. The less stable color centers can be annealed faster than longer lived, more stable color centers by adding energy into the system (actively running the laser). Once the less stable color centers have been annealed, only the longer lived color centers, which are not affected by low temperature annealing, remain. YDF2 received a second dose of gammas on the second day of testing. Following the re-irradiation of YDF2, its active recovery rate

dropped 31% from the recovery rate that same morning before re-irradiation. This suggests that as the total dose increases, the rate at which the YDFL anneals declines significantly. The number of color centers created within the YDFL will increase as it is exposed to higher doses of radiation. Therefore, the recovery time will also increase from the increased number of color centers present in the YDFL.

**Table 5. Active recovery analysis for YDF1 and YDF2.**

| **YDF1 Initial Power: 22 mW** | **Recovery Rate (mW/hr)** | **Time to Full Power Recovery (days)** |
|---|---|---|
| Immediate recovery | 0.23 | 3.84 |
| Next morning recovery | 0.35 | 2.55 |
| Day 5 recovery | 0.11 | 7.77 |
| Day 6 recovery | 0.049 | 15.98 |
| **YDF2 Initial Power: 29 mW** | **Recovery Rate (mW/hr)** | **Time to Full Power Recovery (days)** |
| Immediate recovery | 0.40 | 2.88 |
| Next morning recovery | 0.26 | 4.26 |
| Immediate re-irradiation recovery | 0.079 | 15.18 |
| Day 4 recovery | 0.067 | 17.90 |
| Day 5 recovery | 0.066 | 17.70 |

Dicks published an experiment conducted on an YDFA that was exposed to a 100 krad(Si) dose of gamma radiation from a $^{60}$Co source. The YDFA in Dicks' study experienced a 31% reduction in power from the radiation damage but achieved complete passive recovery of the YDFA after being in room temperature storage for two years [34]. The time line for this thesis prevented an in depth study of passive recovery on the irradiated YDFL due to the significant amount of time passive recovery at room temperature takes.

## 6.5 Conclusions

The comparison of the results presented in this thesis to the literature on radiation sensitivity of RE-doped fibers supports Lezius' conclusions in [6], the same study from Lezius discussed earlier in section 6.1. Predicting how a fiber will be affected by radiation is difficult because radiation sensitivity is dependent on a number of factors including: the dopant elements and concentrations, the co-dopant elements and concentrations, the system configuration (irradiated as a fiber, amplifier, or laser), and the type of radiation the fiber was exposed to [5, 6, 44, 45]. Therefore, actually irradiating the fiber in representative conditions will provide the most accurate results in determining the radiation sensitivity of the fiber. However, the analysis of the results from these experiments indicated that the power law can be used to predict RIA confidently under the gamma irradiation conditions explored in this work (32.7 krad(Si)/hr).

The results from the gamma only and mixed gamma/neutron experiments indicated that the power of the YDFL decreased exponentially with increased radiation dose. The power degradation in these experiments reflected a similar trend to other published results on radiation effects on RE-doped fibers and RE-doped fiber systems (as seen in Table 4). The maximum power loss of the YDFL was 98% for the gamma only experiments, and 77% for the reactor experiments. The initial power of the YDFL in experiment #2 was 7.4 mW higher than in experiment #1, which resulted in less RIA in experiment #2 than in experiment #1. This suggests that a higher initial power for the YDFL prevented the creation of certain color centers within the YDF, reducing RIA.

The power law fit was used to model the RIA in the fiber. The power law fit modeled the experimental results accurately, with fitting results ($R^2$) ranging from 0.9591 - 0.9978 and 0.8885 - 0.9844 for the gamma only and the mixed

gamma/neutron experiments respectively. However, once the total dose exceeded 210 krad(Si) in gamma experiment #3, the RIA from the power law fit was less than the experimental results. This suggests that the fiber dependent variables, $\alpha$ and $\beta$, may need to be adjusted if the total dose will exceed 210 krad(Si). For reactor experiment #1, the data suggests that the dose rate for gamma irradiation was low enough that the power law fit, using the typical constraints on $\alpha$and $\beta$, was not a good model for RIA. Instead, $\beta$ may need to be reduced to less than 0.7 in order to properly model the RIA at gamma dose rates less than 32.7 krad(Si)/hr.

Power recovery experiments were conducted post irradiation with the fiber laser off and actively lasing. The power passively recovered 100 and 550 $\mu$W in 18 and 90 hours respectively. During active recovery the YDFL experienced the same 100 $\mu$W power increase, but in 9.3% of the time (10 min), while the total power recovery was 12.6% and 4.4% for YDF1 and YDF2 respectively. This suggests that active recovery reduced the amount of color centers significantly faster than passive recovery. Another finding was that the active recovery rates declined as the number of days after irradiation increased. This demonstrated that there is a saturation of recovery due to the lifetimes of the color centers in the fiber. The majority of the less stable color centers were annealed in the earlier recovery experiments. As time progressed in active recovery, only the most stable color centers remained, which reduced the power recovery of the YDFL. Finally, comparisons between the total doses of gamma experiments #1 and #2 with #3 showed that as the total dose of the fiber increased, so too did the number of color centers created. This was evidenced by a 31% drop in recovery rate once the fiber was irradiated with gamma radiation for a second time (increasing total dose from 145 to 250 krad(Si)). The number of color centers increased within the fiber as the total dose increased, which ultimately increased the amount of time required to repair these color centers.

The results from the mixed gamma/neutron experiments also showed an exponential decrease of power of the YDFL with increasing radiation dose. The RIA was also calculated for these experiments; the RIA for experiments #1, #2, and #3 were 0.4732, 0.6453, and 6.282 dB/m for total neutron fluences of $5.4\times10^{10}$, $9.1\times10^{12}$, and $1.1\times10^{14}$ n/cm$^2$ respectively. The last neutron fluence resulted in a maximum power loss of 77% for the reactor experiments.

Speculating about the radiation sensitivity of a RE-doped fiber from one type of irradiation experiment, or from an irradiation experiment with the fiber in only one configuration (active, passive, as an amplifier or laser, etc.) would result in inaccurate assumptions. Established databases such as the NEPP Program or the ESCIES, [15, 16], can be used for estimating radiation sensitivity/survivability for applications that are comparable to those contained in these databases. However, if there is variation between the database parameters and the application, the reported RIA may not be an accurate estimation of the RIA that will occur. If an inaccurate assumption is made regarding the radiation sensitivity of the fiber, the survivability of the system in which the fiber is employed may be jeopardized.

### 6.6 Future Research

According to a study performed by Tammela et al., the creation of color centers increased as the percentage of excited $Yb^{3+}$ ions in the YDF increased [46]. Tammela et al. also reported that the solubility of the RE ions could be affected by changing the composition of the silica in which it was doped. More uniformly distributed RE ions decreased the probability of energy migration between the RE ions, which reduced the amount of color centers generated within the fiber [46]. Furthermore, given the same silica composition, increased concentration of RE ions within the silica caused an increase in energy migration probability. Future studies

could be conducted on YDFLs to determine if using longer YDFs that are pumped at lower powers (limiting the amount of population inversion of the $Yb^{3+}$ ions) reduces the amount of RIA seen in the YDFL. This could be achieved by pumping both forwards and backwards in the fiber with two separate pump lasers while irradiating the YDF and monitoring the power *in-situ*. Parallel experiments could be conducted with the same length of YDFs at increased pump power to achieve a greater population inversion. The RIA from both experiments could be compared to determine if there was a reduction of RIA in the YDFs with a lower excited population of $Yb^{3+}$ ions. Recovery experiments could also be conducted to explore if the recovery rate (active or passive) would be affected by utilizing this lower population inversion technique.

Another area in which more research needs to be conducted includes determining the reason why changing the way a specific YDF is configured alters the radiation sensitivity of the fiber. If an YDF is irradiated and shows a specific range of RIA seen in the fiber, what mechanisms are in place that change the radiation sensitivity of the same exact type of YDF when it is used in an YDFA and an YDFL? The benefits of conducting experiments on the same fiber type in all three configurations could help determine which damage mechanisms most affect the fiber in each configuration.

Finally, using a neutron only irradiation source, such as AFITs neutron generator, could help quantify the amount of damage the gamma radiation caused in the mixed neutron/gamma experiments conducted in this thesis. Using a neutron only irradiation source could better isolate how the absorption compares to the absorption seen from gamma only irradiation and a mixed neutron/gamma source, on an active YDFL.

# Bibliography


1. J. Hecht, *Understanding Fiber Optics*, 4th ed. Prentice Hall, 2001.

2. B. Singleton, "Radiation Effects on Ytterbium-Doped Optical Fibers," Ph.D. dissertation, Air Force Insitute of Technology, 2014.

3. Y. Li, J. Huang, Y. Li, H. Li, Y. He, S. Gu, G. Chen, L. Liu, and L. Xu, "Optical properties and laser output of heavily Yb-doped fiber prepared by Sol-Gel method and DC-RTA technique," *Journal of Lightwave Technology*, vol. 26, no. 18, pp. 3256–3260, 2008.

4. Y. Sheng, L. Yang, H. Luan, Z. Liu, Y. Yu, J. Li, and N. Dai, "Improvement of radiation resistance by introducing CeO 2 in Yb-doped silicate glasses," *Journal of Nuclear Materials*, vol. 427, no. 1-3, pp. 58–61, 2012. [Online]. Available: http://dx.doi.org/10.1016/j.jnucmat.2012.04.026

5. H. Henschel, O. Kohn, H. Schmidt, J. Kirchhof, and S. Unger, "Radiation-induced loss of rare earth doped silica fibres," in *RADECS 97. Fourth European Conference on Radiation and its Effects on Components and Systems (Cat. No.97TH8294)*, vol. 45, no. 3. IEEE, 1997, pp. 439–444. [Online]. Available: http://ieeexplore.ieee.org/lpdocs/epic03/wrapper.htm?arnumber=698961

6. M. Lezius, K. Predehl, W. Stower, A. Turler, M. Greiter, C. Hoeschen, P. Thirolf, W. Assmann, D. Habs, A. Prokofiev, C. Ekstrom, T. W. Hansch, and R. Holzwarth, "Radiation Induced Absorption in Rare Earth Doped Optical Fibers," *IEEE Transactions on Nuclear Science*, vol. 59, no. 2, pp. 425–433, apr 2012.

7. G. M. Williams, M. A. Putnam, and B. J. Friebele, "Space Radiation Effects on Er doped fibers," *Proceedings of SPIE*, vol. 2811, pp. 30–37, 1996.

8. M. Ott, "Radiation Effects Expected for Fiber Laser/Amplifier Rare Earth Doped Optical Fiber," Sigma Research and Engineering / NASA GSFC, Parts, Packaging and Assembly Technologies Office, Tech. Rep., 2004.

9. M. Ott, S. Macmurphy, and M. Dodson, "Radiation Testing of Commercial Off the Shelf 62.5/125/250 Micron Optical Fiber for Space Flight Environments," Sigma Research and Engineering, NASA Goddard Space Flight Center, Tech. Rep., 2001.

10. T. S. Rose, D. Gunn, G. C. Valley, and A. Commercially, "Gamma and Proton Radiation Effects in Erbium-Doped Fiber Amplifiers: Active and Passive Measurements," *Journal of Lightwave Technology*, vol. 19, no. 12, pp. 1918–1923, 2001.

11. S. Girard, M. Vivona, A. Laurent, B. Cadier, C. Marcandella, T. Robin, E. Pinsard, A. Boukenter, and Y. Ouerdane, "Radiation hardening techniques for rare-earth based optical fibers and amplifiers," *Optics Express*, vol. 20, no. 8, pp. 8457–8464, 2012.

12. S. Girard, S. Member, L. Mescia, M. Vivona, A. Laurent, Y. Ouerdane, C. Marcandella, F. Prudenzano, A. Boukenter, T. Robin, P. Paillet, V. Goiffon, M. Gaillardin, B. Cadier, E. Pinsard, M. Cannas, and R. Boscaino, "Design of Radiation-Hardened Rare-Earth Doped Amplifers Through a Coupled Experiment/Simulation Approach," *Journal of Lightwave Technology*, vol. 31, no. 8, pp. 1247–1254, 2013.

13. S. Girard, B. Tortech, E. Regnier, M. Van Uffelen, A. Gusarov, Y. Ouerdane,

J. Baggio, P. Paillet, V. Ferlet-Cavrois, A. Boukenter, J. P. Meunier, F. Berghmans, J. R. Schwank, M. R. Shaneyfelt, J. A. Felix, E. W. Blackmore, and H. Thienpont, "Proton- and Gamma-Induced Effects on Erbium-Doped Optical Fibers," *IEEE Transactions on Nuclear Science*, vol. 54, no. 6, pp. 2426–2434, 2007. [Online]. Available: http://ieeexplore.ieee.org/ielx5/23/4394990/04395030.pdf?tp=&arnumber=4395030&isnumber=4394990

14. G. Williams, M. Putnam, C. Askins, M. Gingerich, and E. Friebele, "Radiation effects in erbium-doped optical fibres," *Electronics Letters*, vol. 28, no. 19, p. 1816, 1992.

15. P. N. Program, "NASA Electronic Parts and Packaging (NEPP) Program." [Online]. Available: http://nepp.nasa.gov

16. ESA, "European Space Components Information Exchange System," 2012. [Online]. Available: https://escies.org

17. B. P. Fox, K. Simmons-Potter, S. W. Moore, J. H. Fisher, and D. C. Meister, "Gamma-radiation-induced photodarkening in actively pumped Yb3+-doped optical fiber and investigation of post-irradiation transmittance recovery," *Proceedings of SPIE*, vol. 7434, pp. 74 340C–1–74 340C–9, 2009. [Online]. Available: http://proceedings.spiedigitallibrary.org/proceeding.aspx?articleid=1340845

18. M. Alam, J. Abramczyk, P. Madasamy, W. Torruellas, and A. Sanchez, "Fiber Amplifier Performance in Gamma-Radiation Environment," in *2007 Conference on Optical Fiber Communication and the National Fiber Optic Engineers Conference*. IEEE, mar 2007, pp. 1–3. [Online]. Available: http://ieeexplore.ieee.org/lpdocs/epic03/wrapper.htm?arnumber=4348557

19. J. Bussjager, J. Hayduk, S. T. Johns, and I. P. Consultants, "Comparison of Radiation-Induced Passive and Dynamic Responses in Two Erbium-Doped Fiber Lasers," in *IEEE Aerospace Conference*. IEEE, 2002, pp. 1369–1379.

20. J. Ma, M. Li, L. Tan, Y. Zhou, S. Yu, and Q. Ran, "Experimental investigation of radiation effect on erbium-ytterbium co-doped fiber amplifier for space optical communication in low-dose radiation environment." *Optics Express*, vol. 17, no. 18, pp. 15 571–15 577, 2009.

21. F. Mady, M. Benabdesselam, Y. Mebrouk, and B. Dussardier, "Radiation effects in ytterbium-doped silica optical fibers: traps and color centers related to the radiation-induced optical losses," *Radecs 2010 Proceedings*, pp. 1–4, 2010.

22. S. Jetschke, U. Röpke, S. Unger, and J. Kirchhof, "Characterization of photodarkening processes in Yb doped fibers," in *Proceedings of SPIE*, D. V. Gapontsev, D. A. Kliner, J. W. Dawson, and K. Tankala, Eds., vol. 7195, feb 2009, pp. 71 952B–1–71 952B–12. [Online]. Available: http://proceedings.spiedigitallibrary.org/proceeding.aspx?articleid=1332888

23. "John Tyndall experiment," 2015. [Online]. Available: http://www.fomsn.com/wp-content/uploads/2015/04/john-tyndall-light-can-be-guided-experiment.png

24. A. Bjarklev, *Optical fiber amplifiers: design and system applications*. Artech House, 1993.

25. M. J. F. Digonnet, *Rare-earth-doped fiber lasers and amplifiers*. CRC Press, 2001.

26. H. Pask, R. Carman, D. Hanna, A. Tropper, C. Mackechnie, P. Barber, and J. Dawes, "Ytterbium-doped silica fiber lasers: versatile sources for the 1-1.2 $\mu$m region," *IEEE Journal of Selected Topics in Quantum Electronics*, vol. 1,

no. 1, pp. 2–13, 1995. [Online]. Available:
http://ieeexplore.ieee.org/lpdocs/epic03/wrapper.htm?arnumber=468377

27. E. Hecht, *Optics*, 4th ed. Reading MA: Addison-Wesley Publishing Company, 2001.

28. "Lasers: Fundamentals." [Online]. Available: http://www.optique-ingenieur.org/en/courses/OPI_ang_M01_C01/co/Contenu_05.html

29. B. Mellish, "A three-level laser energy diagram." [Online]. Available: https://en.wikipedia.org/wiki/Population_inversion

30. C. Diehl, "Constructing A High Power Single-mode Fiber Laser," Bachelor's Thesis, Robert D. Clark Honors College, 2014.

31. Grahamwild, "Polarization independent isolator." [Online]. Available: https://en.wikipedia.org/wiki/Optical_isolator

32. A. M. Fox, *Optical Properties of Solids*, ser. Oxford master series in condensed matter physics. Oxford University Press, 2001. [Online]. Available: https://books.google.com/books?id=-5bVBbAoaGoC

33. J. J. Koponen, M. J. Söderlund, S. K. T. Tammela, and H. Po, "Photodarkening in ytterbium-doped silica fibers," *Proceedings of SPIE*, vol. 5990, pp. 599 008–1–599 008–10, 2005. [Online]. Available: http://proceedings.spiedigitallibrary.org/proceeding.aspx?articleid=1333313

34. B. M. Dicks, F. Heine, K. Petermann, and G. Huber, "Characterization of a Radiation-Hard Single-Mode Yb-Doped Fiber Amplifier at 1064 nm," *Laser Physics*, vol. 11, no. 1, pp. 134–137, 2001.

35. L. Rumbaugh, "Fiber Lasers and Amplifiers Design Toolbox - File Exchange," 2013. [Online]. Available: http://www.mathworks.com/matlabcentral/fileexchange/42122-fiber-lasers-and-amplifiers-design-toolbox

36. J. R. Taylor, *An Introduction to Error Analysis*. University Science Books, 1997.

37. S. Moore, T. Barnett, T. Reichardt, and R. Farrow, "Optical properties of Yb+3-doped fibers and fiber lasers at high temperature," *Optics Communications*, vol. 284, no. 24, pp. 5774–5780, 2011.

38. B. P. Fox and Z. V. Schneider, "Gamma Radiation Effects in Yb-Doped Optical Fiber," *Proceedings of SPIE*, vol. 6453, 2007.

39. B. P. Fox, K. Simmons-Potter, W. J. Thomes, and D. a. V. Kliner, "Gamma-radiation-induced photodarkening in unpumped optical fibers doped with rare-earth constituents," *IEEE Transactions on Nuclear Science*, vol. 57, no. 3 Part 3, pp. 1618–1625, 2010.

40. E. J. Griscom, D L., Gingerich, M. E., Friebele, "Radiation-Induced Defects in Glasses: Origin of Power-Law Dependence of Concentration on Dose," *Physical Review Letters*, vol. 71, no. 7, pp. 1019–1022, 1993.

41. J. Koponen, M. Laurila, M. Söderlund, J. J. Montiel i Ponsoda, and A. Iho, "Benchmarking and measuring photodarkening in Yb doped fibers," *Proceedings of SPIE*, vol. 7195, pp. 71 950R–1–71 950R–14, 2009. [Online]. Available: http://proceedings.spiedigitallibrary.org/proceeding.aspx?articleid=1332832

42. R. G. Ahrens, J. J. Jaques, M. J. Luvalle, D. J. Digiovanni, and R. S. Windeler, "Radiation effects on optical fibers and amplifiers," *Proceedings of SPIE*, vol. 4285, pp. 217–225, 2001.

43. S. Girard, Y. Ouerdane, M. Vivona, B. Tortech, T. Robin, A. Boukenter, C. Marcandella, B. Cadier, and J.-P. Meunier, "Radiation effects on rare-earth doped optical fibers," *Proceedings of SPIE*, vol. 7817, no. May 2011, pp. 78 170I–1–78 170I–10, 2010. [Online]. Available: http://link.aip.org/link/PSISDG/v7817/i1/p78170I/s1&Agg=doi

44. E. W. Taylor and J. Liu, "Ytterbium-doped fiber laser behavior in a gamma-ray environment," *Proceedings of SPIE*, vol. 5897, pp. 58 970E–1–58 970E–9, 2005.

45. C. E. Barnes, M. N. Ott, A. H. Johnston, K. A. LaBel, R. A. Reed, C. J. Marshall, and T. Miyahira, "Recent Photonics Activities Under the NASA Electronic Parts and Packaging (NEPP) Program," in *Proceedings of SPIE*, E. W. Taylor, Ed., vol. 4823, no. 818, 2002, pp. 189–204.

46. S. Tammela, M. Söderlund, J. Koponen, V. Philippov, and P. Stenius, "The potential of direct nanoparticle deposition for the next generation of optical fibers," *Proceedings of SPIE*, vol. 6116, pp. 61 160G–1–61 160G–9, 2006. [Online]. Available: http://dx.doi.org/10.1117/12.660405

# REPORT DOCUMENTATION PAGE

*Form Approved*
*OMB No. 0704-0188*



| 1. REPORT DATE *(DD-MM-YYYY)* | 2. REPORT TYPE | 3. DATES COVERED *(From - To)* |
|---|---|---|
| 24-03-2016 | Master's Thesis | Sep 2014 - Mar 2016 |

**4. TITLE AND SUBTITLE**
Radiation Effects on an Active Ytterbium-doped Fiber Laser

**5a. CONTRACT NUMBER**

**5b. GRANT NUMBER**

**5c. PROGRAM ELEMENT NUMBER**

**6. AUTHOR(S)**
Poulin, Adam C., Capt, USAF

**5d. PROJECT NUMBER**
15P933

**5e. TASK NUMBER**

**5f. WORK UNIT NUMBER**

**7. PERFORMING ORGANIZATION NAME(S) AND ADDRESS(ES)**
Air Force Institute of Technology
Graduate School of Engineering and Management (AFIT/EN)
2950 Hobson Way
Wright-Patterson AFB OH 45433-7765

**8. PERFORMING ORGANIZATION REPORT NUMBER**
AFIT-ENP-MS-16-M-079

**9. SPONSORING/MONITORING AGENCY NAME(S) AND ADDRESS(ES)**

Defense Threat Reduction Agency
Maj Michael Pochet
8725 John. J. Kingman Rd
Ft. Belvoir, VA 22060
michael.c.pochet.mil@mail.mil

AFIT Faculty Research Council
Dr. Heidi Ries
2950 Hobson Way
WPAFB OH 45433-7765
heidi.ries@us.af.mil

**10. SPONSOR/MONITOR'S ACRONYM(S)**
DTRA, AFIT FRC

**11. SPONSOR/MONITOR'S REPORT NUMBER(S)**

**12. DISTRIBUTION/AVAILABILITY STATEMENT**
DISTRIBUTION STATEMENT A:
APPROVED FOR PUBLIC RELEASE; DISTRIBUTION UNLIMITED.

**13. SUPPLEMENTARY NOTES**
This work is declared a work of the U.S. Government and is not subject to copyright protection in the United States.

**14. ABSTRACT**

This is the first published research focused on the impact of gamma and mixed gamma/neutron radiation on an actively lasing ytterbium-doped fiber laser. While the gain medium of the laser was irradiated, the power was measured in-situ and the spectrum was recorded intermittently. The results indicate that as the total dose increased linearly with time, the laser experienced an exponential decay in power with a maximum power loss of 99.84%, and the lasing wavelength blueshifted up to 15 nm. The laser, when exposed to 145 krad(Si), experienced less attenuation with a higher initial power than with a lower initial power. Power recovery experiments were conducted post-irradiation with the fiber laser off and actively lasing. Passively, the power recovered 100 and 550 uW in 18 and 90 hours respectively. Active recovery experienced the same 100 uW recovery in 9.3% of the time (10 min), and total power recovery of 12.6% and 4.4% for YDF1 and YDF2 respectively. The active recovery rate declined as the number of days following irradiation increased, indicating a saturation of recovery from less stable color centers being repaired.

**15. SUBJECT TERMS**
Ytterbium-doped fiber laser, gamma irradiation, neutron irradiation, active annealing, doped fiber laser, rare earth doped fiber laser, radiation induced attenuation, Ytterbium-doped fiber, in-situ

| 16. SECURITY CLASSIFICATION OF: | | | 17. LIMITATION OF ABSTRACT | 18. NUMBER OF PAGES | 19a. NAME OF RESPONSIBLE PERSON |
|---|---|---|---|---|---|
| a. REPORT | b. ABSTRACT | c. THIS PAGE | | | Briana J. Singleton, Lt. Col,, Ph.D., AFIT/ENP |
| U | U | U | UU | 103 | 19b. TELEPHONE NUMBER *(Include area code)* (937) 255-3636 x4571 briana.singleton@afit.edu |